ISTANBUL TECHNICAL UNIVERSITY ★ GRADUATE SCHOOL

DESIGN AND DEVELOPMENT OF PVA/HYDROCORTISONE LOADED XEROGEL NANOFIBROUS MAT FOR TOPICAL DRUG DELIVERY

M.Sc. THESIS

Hisham Ali Muhammad Ali MOUSSA

Department of Textile Engineering

Textile Engineering Programme

JUNE 2023

ISTANBUL TECHNICAL UNIVERSITY ★ GRADUATE SCHOOL

DESIGN AND DEVELOPMENT OF PVA/HYDROCORTISONE LOADED XEROGEL NANOFIBROUS MAT FOR TOPICAL DRUG DELIVERY

M.Sc. THESIS

Hisham Ali Muhammad Ali MOUSSA
(503201811)

Department of Textile Engineering

Textile Engineering Programme

Thesis Advisor: Prof. Dr. Burçak KARAGÜZEL KAYAOĞLU

JUNE 2023

İSTANBUL TEKNİK ÜNİVERSİTESİ ★ LİSANSÜSTÜ EĞİTİM ENSTİTÜSÜ

TOPİKAL İLAÇ SALINIMI İÇİN PVA/HİDROKORTIZON İLE YÜKLÜ KSEROJEL NANOLİF YÜZEY TASARIMI VE GELİŞTİRİLMESİ

YÜKSEK LİSANS TEZİ

Hisham Ali Muhammad Ali MOUSSA
(503201811)

Tekstil Mühendisliği Anabilim Dalı

Tekstil Mühendisliği Programı

Tez Danışmanı: Prof. Dr. Burçak KARAGÜZEL KAYAOĞLU

HAZİRAN 2023

Hisham Ali Muhammad Ali MOUSSA, a M.Sc. Student of ITU Graduate School student ID 503201811, successfully defended the thesis entitled "DESIGN AND DEVELOPMENT OF PVA/HYDROCORTISONE LOADED XEROGEL NANOFIBROUS MAT FOR TOPICAL DRUG DELIVERY", which he prepared after fulfilling the requirements specified in the associated legislations, before the jury whose signatures are below.

Thesis Advisor:	**Prof. Dr. Burçak KARAGÜZEL KAYAOĞLU** İstanbul Technical University
Jury Members:	**Prof. Dr. Levent Trabzon** İstanbul Technical University
	Dr. Öğr. Üyesi Nuray KIZILDAĞ Gebze Technical University

Date of Submission : 16 May 2023
Date of Defense : 16 June 2023

To my dearest wife,

FOREWORD

I am eternally grateful to my advisor Prof. Dr. Burçak Karagüzel Kayaoğlu for her guidance, encouragement and patience during my thesis study. I would like to thank Merkas Textile for providing the necessary materials. Selahattin Onur, R&D Manager in Merkas Textile, for his support of the study. I also would like to sincerely thank Dr. Özlem İpek Kalaoğlu for always being there when I needed any help or advice during the course of my thesis study, I would also like to express my thanks to Res. Asst. Handan Palak for teaching me and helping throughout my study. Lastly, I would like to thank Istanbul Technical University Scientific Research Projects Fund under Grant No. BAP 43318 for the financial support.

Without all of them, I could have not completed this MSc. study.

June 2023

Hisham Ali Muhammad Ali MOUSSA
(Textile Engineer)

TABLE OF CONTENTS

Page

ABBREVIATIONS

PVA	: Poly(vinyl alcohol)
PVA/hydrocortisone	: PVA loaded with hydrocortisone
PVA/xerogel/hydrocortisone	: PVA and hydrocortisone loaded xerogel
pH	: potential of hydrogen
CO_2	: Carbon dioxide
TMOS	: Tetramethyl orthosilicate
NH_4OH	: Ammonium hydroxide
PBS	: Phosphate buffer saline 7.4
UV-Vis	: Ultraviolet–visible
BET	: Brunauer-Emmett-Teller
BJH	: Barrett-Joyner-Halenda
SEM	: Scanning Electron Microscopy
EDAX	: Energy-dispersive X-ray spectroscopy
FTIR	: Fourier Transform Infrared Spectroscopy

SYMBOLS

A	**:** Absorbance
L	**:** Optical path length
C	**:** Concentration
ε	**:** Molar extinction coefficient
I_o	**:** Incident intensity
I	**:** Transmitted intensity
R^2	**:** Slope and coefficient of determination
Au	**:** Gold
Pd	**:** Palladium
Si	**:** Silicone
O	**:** Oxygen
Al	**:** Aluminum
C	**:** Carbon
H	: Hydrogen

LIST OF TABLES

Page

LIST OF FIGURES

Page

DESIGN AND DEVELOPMENT OF PVA/HYDROCORTISONE LOADED XEROGEL NANOFIBROUS MAT FOR TOPICAL DRUG DELIVERY

SUMMARY

Textile materials have always been utilized in the medical field. The unique properties they offer, biocompatibility and versatility are the major reasons behind that. They can be found in applications ranging from a simple bandage to full on blood vessels. Nanofiber-based textile materials are textile materials known for their high surface area and interconnected porosity. Nanofiber- based textile materials can be fabricated with a variety of methods yet; the most dominant method is electrospinning. Furthermore, in the recent years there has been a rise of interest in different materials as well such as; aerogels.

Aerogels are porous materials that have unique properties that make them good candidates for drug careering and releasing. Aerogels can be made of different materials such as polymers, biopolymers and metal oxides but the most common types of aerogels are silica, carbon and metal oxide aerogels. The process of synthesizing aerogel consists mainly of three stages; gelation, aging and drying. The process of drying aerogels affects the synthesized aerogel greatly as you can have three different types of aerogels by just using a different drying technique. Xerogel is one of the types of aerogels and it is achieved by drying aerogels at ambient pressure.

This study aimed to design and develop a PVA/hydrocortisone loaded xerogel electrospun mat for topical drug delivery. The silica xerogel was synthesized using TMOS as a silica precursor, Ammonium hydroxide as a catalyst and Methanol as a co-solvent. The xerogel was ball-milled into fine powder and had its surface area, pore size and volume analyzed. In addition to that, hydrocortisone was loaded into three different samples; one consisting of only xerogel, the second of only PVA nanofibrous mat and the third consisting of both xerogel and PVA nanofibrous mat. In vitro drug release analysis was carried out for all of these samples. PVA was chosen for its biocompatible properties and stability. SEM and EDAX analyses were carried out to investigate the surface of the fibers and elements existing in the samples respectively. In addition to that, FTIR analysis was performed to identify the different materials making up the nanofibrous mats.

The synthesized silica xerogel had a surface area of around 505 m^2/g, pore size of around 3.8 nm and a pore volume of 0.48 cm^3/g. SEM images showed the hydrocortisone loaded xerogel inside the PVA nanofibrous mat and the EDAX analysis confirmed the existence of silicone in the samples due to the existence of silica xerogel as well as a high concentration of Carbon due to hydrocortisone. The hydrocortisone loaded xerogel showed a slow sustained drug delivery release behavior and around 69.3% of the loaded hydrocortisone was released in 25 days. The PVA/xerogel/hydrocortisone nanofibrous mat showed a similar drug release behavior with a release of around 79.2% of the hydrocortisone initially loaded with PVA was released in just 30 minutes. Demonstrating a conventional or retarded drug release behavior. Meanwhile, the PVA/hydrocortisone electrospun mat showed a completely

different drug release behavior. Around 98.55% of the hydrocortisone initially loaded into the PVA.

In conclusion, Silica xerogel as a drug carrier was successfully synthesized. It was loaded with hydrocortisone. Hydrocortisone loaded silica xerogel drug release was investigated as well as PVA/xerogel/hydrocortisone and PVA/hydrocortisone. The result of these three different sample types were collected and compared. Both hydrocortisones loaded xerogel and PVA/xerogel/hydrocortisone showed a slow sustained drug release behavior. Meanwhile PVA/hydrocortisone showed a retarded drug release behavior. These results suggest the capability of PVA/hydrocortisone load xerogel mat to work as a sustained/controlled topical drug delivery carrier.

TOPİKAL İLAÇ VERİLMESİ İÇİN HİDROKORTIZON İLE YÜKLÜ KSEROJELİN TASARIMI VE GELİŞTİRİLMESİ

ÖZET

Medikal alanda tekstil malzemeleri elyaf, iplik, dokuma, örme veya dokusuz kumaşlar şeklinde uzun süredir varlığını sürdürür. Bu yüksek çok yönlülük, tekstil malzemelerinin tıbbi alanda bandajlardan tam yapay kan damarlarına kadar pek çok uygulamada bulunmasına önemli bir katkı sağlamaktadır.

Günümüzde tekstil malzemelerinin medikal alanda kullanımı, tekstil malzemeleri fabrikasyon teknolojilerinin gelişmesi ile artmaktadır. Bu kullanım artışı diğer tekstil malzemeleri formlarında da gözlemlenebilir olsa da, nanoliflerden yapılan tekstil malzemeleri başı çeker. Bunun başlıca nedeni, nanofiber bazlı tekstil malzemelerini tıbbi uygulamalar için ideal hale getiren diğer birçok özelliğin yanı sıra yüksek spesifik yüzey alanları ve birbirine bağlı gözenekliliktir. Aerojeller son zamanlarda çok fazla ilgi gördü. Bu kısmen, bu malzemelerin sağladığı benzersiz özelliklerden ve çok yönlülüklerinden kaynaklanmaktadır; araştırma yapmak ve birçok uygulamaya dahil etmek için çekici bir malzeme haline geldiler.

Aerojeller, yüksek gözenekli bir yapıya sahip, düşük yoğunluklu, açık hücreli malzemelerdir. Bu mikro yapı, aerojele son derece düşük termal iletkenlik, yüksek gözeneklilik ve yüzey alanı gibi olağanüstü bir özellik kazandıran oldukça kıvrımlı bir nanoparçacık ağı oluşturur. Pek çok aerojel türü vardır, ancak en yaygın olanları silis, karbon ve metal oksitlerden yapılanlardır. Bu üç tip arasında silika aerojel açık bir farkla en çok kullanılan aerojel türüdür. Karbondan yapılan aerojeller, esas olarak yakıt hücreleri ve süper kapasitörler için kullanılırken metal oksitlerden yapılan aerojeller, daha çok katalizörler ve karbon nanotüp üretiminde kullanılır. Öte yandan, silika aerojeller, havanın yarısı kadar termal iletkenliğe sahip oldukları için ve çoğunlukla ısı yalıtımı için kullanıldıkları için, çok düşük termal iletkenliklerinden yararlanırlar.

Silika aerojeller, geniş çapta ve en yaygın olarak üretilen aerojellerdir. Sentezleme işlemi başlıca üç ana aşamadan oluşur: jelleşme, eskitme ve kurutma. Jelleşme, silika jelin, bir jelleşme katalizörünün eklenmesi yoluyla kararlı bir silika nanoparçacıklarının kararsız hale gelmesinin meydana geldiği ve dolayısıyla pH'ını değiştirerek yüzey yükünü değiştirdiği bir sol-jel işlemi tarafından üretildiği aşamadır. Bu aşamada ana parçacıklar oluşur ve kümeler halinde birleştirilir, ardından inci kolyeyi andıran bir yapıda kesişir. Eskitme, ilk adımda hazırlanan jelin, stok solüsyonunda eskitildiği jelleşmeden sonra gelir. Son aşama, çoğu kişi tarafından sentez sürecindeki en kritik adım olarak kabul edilen kurutmadır. Silika aerojellerin kurutulabildiği farklı teknikler vardır ve her teknik kısmen farklı özelliklere sahip farklı tipte bir aerojel ile sonuçlanır.

En yaygın kurutma tekniği süperkritik kurutmadır. Bu, buharlaşma sırasında yüksek kapileri önlemek için yapılır. Kaçınılmazsa gözeneklerin çökmesine neden olabilir. Kritik noktası 31◦C ve 73 bar olan CO_2'ye dayalı süperkritik sıvı olarak CO2'nin

kullanılması, toplu doğa sürecine rağmen artık endüstriyel üretimde en yaygın yaklaşımdır. Bu teknikler, farklı şekil ve boyutlarda kalıplanabilen ve aerojelin gözeneklerini sağlam tutan katı bir aerojel üretir. Yüzey alanı bakımından en gözenekli ve aynı zamanda en yüksek olanıdır.

İkinci teknik dondurarak kurutmadır. Bu kurutma işlemi, kriyojel adı verilen özel bir aerojel türü üretir. Bu kriyojeller, başlangıç çözücüsüne ve öncü konsantrasyonlarına bağlı olarak mikro ölçekten sıcaklık ve donma hızına kadar değişen gözenek boyutlarına sahip olabilir.

Son kurutma tekniği, daha çok endüstriyel ölçekte silika aerojel granül ve toz üretmek için kullanılan ortam basınçlı kurutmadır. Kılcal kuvvetler ve büzülme, ortam basıncında kuruma boyunca gerçekleşir, ancak bazı yüzey modifikasyonları ve eskime ile kontrol altında tutulabilir. Bu yöntem, süper kritik derecede kurutulmuş aerojele kıyasla daha yoğun olan ve kserojel olarak bilinen bir aerojel türünü üretir.

Kserojeller, aerojellerin özel bir şeklidir. Sol-jel, ortam koşullarında kurutulduğunda elde edilirler. Kserojeller, aerojeller gibi gözenekli malzemelerdir. Ortamda kurutulmuş, çapraz bağlı polimerik ağlardan yapılmıştır. Yüksek gözeneklilik, yüksek yüzey alanı gibi aerojellere benzer, ancak daha az karmaşık ve çok daha ucuz üretim maliyetine sahip özelliklere sahiptirler. Aerojellere benzer şekilde, Kserojeller organik veya inorganik öncülerden hazırlanabilir. Kserojellerin en dikkate değer avantajı, uyluktan ilaç yükleme kapasitesi ve sürekli bir ilaç salımını sürdürme yeteneğidir. Ayrıca biyouyumludurlar ve toksik değildirler, bu da kserojelleri birçok biyomedikal uygulama için uygun hale getirir.

İlaç verme, belirli bir ilacın veya bileşiğin verilme şeklidir.Yıllar boyunca birçok ilaç dağıtım sistemi geliştirilmiştir. Başlıca üç tip ilaç salım mekanizması vardır. Konvansiyonel salım, yani ilacın salımının anlık bir hızda hemen gerçekleştiği ani salım, bu nedenle anında salım adı verilir. İkinci tip, ilacın belirli bir süre boyunca yavaş salınımını tanımlayan sürekli salınımdır. Üçüncü tip kontrollü salım olup, aynı zamanda ilacın yavaş, ancak öngörülebilir ve programlanmış bir hızda salınmasını da tanımlar.

Bu çalışma, topikal ilaç uygulaması için hidrokortizon yüklü kserojel tasarlamayı ve geliştirmeyi amaçlamıştır. Silika kserojel, silika öncüsü olarak, TMOS katalizör olarak ,Amonyum hidroksit ve yardımcı çözücü olarak Metanol kullanılarak sentezlenmiştir. Kserojel bilyeli öğütülerek ince toz haline getirilmiş ve yüzey alanı, gözenek boyutu ve hacmi analiz edilmiştir. Bunlara ek olarak, hidrokortizon kserojele, PVA nanolifli mat PVA/hidrokortizona ve kserojel bir PVA nanolifli matın (PVA/hidrokortizon yüklü kserojel) içine yüklenmiştir. Bu numunelerin tümü için in vitro ilaç salım analizi gerçekleştirilmiştir. PVA, biyouyumlu özellikleri ve kararlılığı nedeniyle seçilmiştir. Örneklerde bulunan liflerin ve elementin yüzeyini araştırmak için SEM ve EDAX analizleri yapılmıştır. Ek olarak, nanolifli matlardaki malzemeleri tanımlamak için FTIR analizi yapılmıştır.

Sonuç, silika öncü çözeltisi olarak TMOS, katalizör olarak NH_4OH ve yardımcı çözücü olarak Metanol kullanılarak başarılı bir Silika kserojel sentezini gösterdi. Sentezlenen silika kserojeller, özellikleri üzerinde herhangi bir olumsuz etki olmaksızın bir bilyalı değirmende 15-20 dakika boyunca 30hz'de başarılı bir şekilde öğütüldü. Sentezlenen silika xerojel tozunun yüzey alanı 505 m^2/g, gözenek hacmi 0.48 cm^3/g idi. Ortalama gözenek boyutu 3.8nm, nanoparçacık boyutu 11.8nm ve medyan gözenek genişliği 0.68nm.

Hidrokortizon, 1:2 oranında silis kserojele başarıyla yüklendi ve iki elektrodöndürme numunesi elektro eğirme işlemine tabi tutuldu; biri hidrokortizon yüklü PVA'dan (PVA/hidrokortizon), ikincisi PVA ve hidrokortizon yüklü kserojelden (PVA/hidrokortizon yüklü kserojel) oluşur. Akış hızı 1.0mL/sa, voltaj 20kV ve toplayıcı ile iğne ucu arasındaki mesafe 15 cm olanların imalatında elektroeğirme kullanıldı. SEM sonuçları, PVA/hidrokortizon yüklü kserojelde hidrokortizon yüklü kserojel varlığını gösterirken, PVA/hidrokortizon numunesinde hidrokortizonun saptanmasının zor olduğunu gösterdi. Bu sırada EDAX sonuçları, diğer numunenin yanı sıra PVA/hidrokortizon yüklü kserojel örneğinde kserojel ve hidrokortizonun varlığını gösterdi. Buna ek olarak, her iki örneğin FTIR analizi EDAX bulgularını destekledi.

Hidrokortizon yüklü kserojel için yapılan laboratuvar ortamında ilaç salım çalışması, hidrokortizonun başlangıçta kserojelden hızlı bir oranda salındığını, ancak bundan sonra salınmanın daha yavaş ve sürekli hale geldiğini ve kserojel içine yüklenen başlangıçtaki hidrokortizon miktarının %69,3'ünün 25 gün içinde salındığını gösterdi. Ayrıca, PVA/hidrokortizon yüklü kserojel için laboratuvar ortamında ilaç salım çalışması, hidrokortizon yüklü kserojelinkine benzer bir davranış gösterdi ve kserojele yüklenen başlangıç hidrokortizon miktarının %79,2'si 25 gün içinde salındı. Bu arada, hidrokortizon yüklü PVA için yapılan laboratuvar ortamında ilaç salım çalışması, geleneksel/geciktirilmiş bir ilaç salım davranışı gösterdi ve PVA'ya yüklenen başlangıç hidrokortizon miktarının %98,55'i 30 dakika içinde salındı.

1. INTRODUCTION

Textile materials in the medical field have existed for a long time. Either in the form of fibers, yarn, woven, knitted or nonwoven fabrics. This high versatility is a major contributor to the textile materials being present in the medical field in so many applications ranging from bandages to full artificial blood vessels.

Today the utilization of textile materials in the medical field increases with the advancement of textile materials fabrication technologies. Although this increase of utilization can be observed with other forms of textile materials, textile materials made of nanofibers come on top. This is mainly due to their high specific surface area, interconnected porosity among many other properties that make nanofiber-based textile materials ideal for medical applications.

Aerogels have had a lot of attraction lately. This is in part due to the unique properties that these materials provide and their versatility; they have become an attractive material to investigate and incorporate into many applications. Looking back at the last decade, there are a clear growing interest of aerogels in the scientific research field especially in drug loading and release which is made obvious by the growing number of published researches (J. Yang et al., 2019; C.A. García-Gonz´alez et al., 2015).

There are many types of aerogels but the most common ones are those made of silica, carbon and metal oxides. Between those three types, silica aerogel is by far the most used type of aerogel. Aerogels made of carbon are mainly used for fuel cells and supercapacitors. Aerogels made of metal oxides are used mainly in catalysts and carbon nanotubes production. On the other hand, silica aerogels take advantage of their very low thermal conductivity, as they have a thermal conductivity half that of air and are mainly used for thermal insulation.

Despite that, silica aerogels can be and have been utilized in many other fields. One of those fields is the biomedical field and drug delivery to be specific. Drug delivery systems has a set of requirements that many types of aerogels do meet. There have been multiple studies on the use of aerogels in the field of oral drug delivery as well as their diffusion of different types of drugs (Sieminska L et al.,1997).

Drug delivery is the way in which a specific drug or compound is given. Throughout the years, many drug delivery systems have been developed. Drug Delivery can either be categorized depending on the release behavior such as immediate drug delivery, sustained drug delivery or controlled drug delivery etc. or it can be categorized depending on the administration method used such as oral drug delivery, topical drug delivery and transdermal drug delivery etc. One of these types of drug delivery systems goes back centuries ago. Going back to ancient Egyptians, there were medicines made of different plants, herb or minerals and were used as topical drugs. They were used by either getting rubbed or applied on skin (Ebbell B., 1937). Ibn Sina also describes in his book The Canon of Medicine, that topical drugs essentially have two different states. One is described as soft and goes through the skin and the other one is hard and does not go through (Moghimi H.R et al., 2011). This lays the foundation of the present-day knowledge of topical and transdermal drug delivery systems.

The skin of humans consists of three layers. These layers are epidermis, dermis and hypodermis. Topical drug delivery treats locally. It does not have an effect past the epidermis layer. unlike, transdermal drug delivery which pass through skin layers into the blood circulation itself.

Combining nanofibrous textile materials and aerogels in a drug delivery system would allow that system to take advantage of the high surface area that comes of the nanofibrous textile materials and the aerogels as well. Furthermore, the drug can be carried within nanofibers themselves or within the aerogel itself which in turns affect the cumulative release of the carried drug.

1.1 Objectives and Novelty of the Study

In this study the aim was to synthesis silica xerogel, investigate its capability for hydrocortisone carrying as well as releasing in specific environment. Silica xerogel was also incorporated into an electrospun mat consisting of Poly(vinyl alcohol) (PVA). This electrospun PVA mat with hydrocortisone loaded xerogel (PVA/xerogel/hydrocortisone) were analyzed for its hydrocortisone release and compared verses the hydrocortisone release in xerogel as well as in PVA nanofibrous mat loaded with hydrocortisone (PVA/hydrocortisone). While previous work focused mainly on xerogel for oral drug delivery, which showed a lot of promise. Here we expand on that and we shift the focus on utilizing the properties of silica xerogel inside

an electrospun mat and investigating its drug release inside a topical drug delivery system.

The literature review indicated that silica xerogel is more than capable of carrying drugs – steroids to be exact – but it was purely for oral drug delivery and it has not been integrated into an electrospun mat for topical drug delivery or wound dressing. Therefore, this study aims to add to the literature by analyzing the performance of the silica xerogel as a drug carrier inside an electrospun mat and comparing it to the performance of the silica xerogel by itself. In addition to that a comparison between the use of xerogel as a drug carrier and its drug release with purely using the PVA electrospun mat as the carrier with no xerogel involved. The data provided from this study could help pave the way forward for the use of silica xerogel in topical drug delivery applications.

2. LITERATURE REVIEW

2.1 Aerogels

Solid, liquid and gas. These are the three commonly known states of matter. As shown in Figure 2.1, aerogels fall into the gap between the liquid and gas state (Du, A., et al., 2013). Aerogels are type of materials that have three-dimensional open networks congregated by polymer molecules (Fricke, J., 1988; Fricke, J. et al., 1998; Pierre, A.C et al., 2002; Vacher, R. et al., 1988). Given this information, aerogels are considered by some as a new state of matter not just a new material (Wagh, P. Et al., 1999). Aerogels just like solid state matters keep up a fixed shape and volume. Yet, their density could be lower than the density of the air, which in turns affect its properties. (Fricke, J. Et al., 1998; Pierre, A.C et al., 2002; Schaefer et al., 1986; Gesser, H. Et al., 1989).

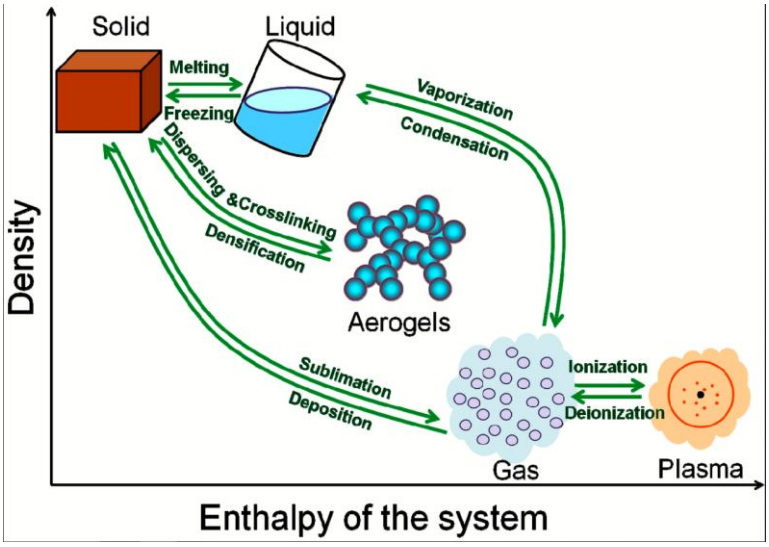

Figure 2. 1 : Distribution and transition of different states of matter. (Du, A., et al., 2013).

Aerogels are defined as low dense, open-cell materials that packs a high porous structure (S.S. Kistler, 1931; N. Hüsing et al., 1998; A.C. Pierre et al., 2011). This structure or rather say, microstructure creates a rather convoluted network of nanoparticles which in turn gives the aerogel an extraordinary property, such as extremely low thermal conductivity, high porosity and surface area. An aerogel is a material generated from the process of replacing the liquid inside a gel with a gas (C.A. García-Gonz´alez, et al., 2019). It is similar to the hydrogels yet the main difference is aerogels have a much higher degree of swelling compared to hydrogels. Aerogels can be generated from a wide variety of materials, including polymers, biopolymers, and even metal oxides. Aerogel made out of Silica are the most common aerogel in the market due to its production value and real-world applications (J.P. Arenas et al., 2010).

2.1.1 Silica aerogel synthesis

Silica aerogels are the most common and widely produced aerogels and the process of synthesizing mainly consists of three main stages: gelation, aging and drying. Gelation is the stage at which the silica gel is produced by a sol-gel process where a destabilizing of stable silica nanoparticles occurs through the addition of a gelation catalyst therefore changing its surface charge by changing its potential of hydrogen (pH). During that stage the main particles are formed and then combined into clusters, and then intersect in a structure resembling a pearl necklace (Karout A et al., 2007), as shown in Figure 2.2.

Aging comes after gelation where the gel prepared in the first step is aged in its stock solution. Many studies have been done on the effects and importance of this step but its main purpose is strengthening the gel by strengthening the particle necks which it turns reduces shrinkage during the drying process. Studies also showed that aging the silica aerogels within its gelation is sufficient enough to strengthens the gel network of silica aerogels if dried by ambient pressure drying liquid making the solvent exchange not necessary. Another big factor of Aging is time. Although aging silica aerogels for days and weeks can be considered impractical for industrial silica aerogel production, aging time can be reduced if done under higher temperatures (Subramaniam Iswar et al., 2017). Table 2.1 shows the effects of aging time and temperature on the physical properties of silica aerogel.

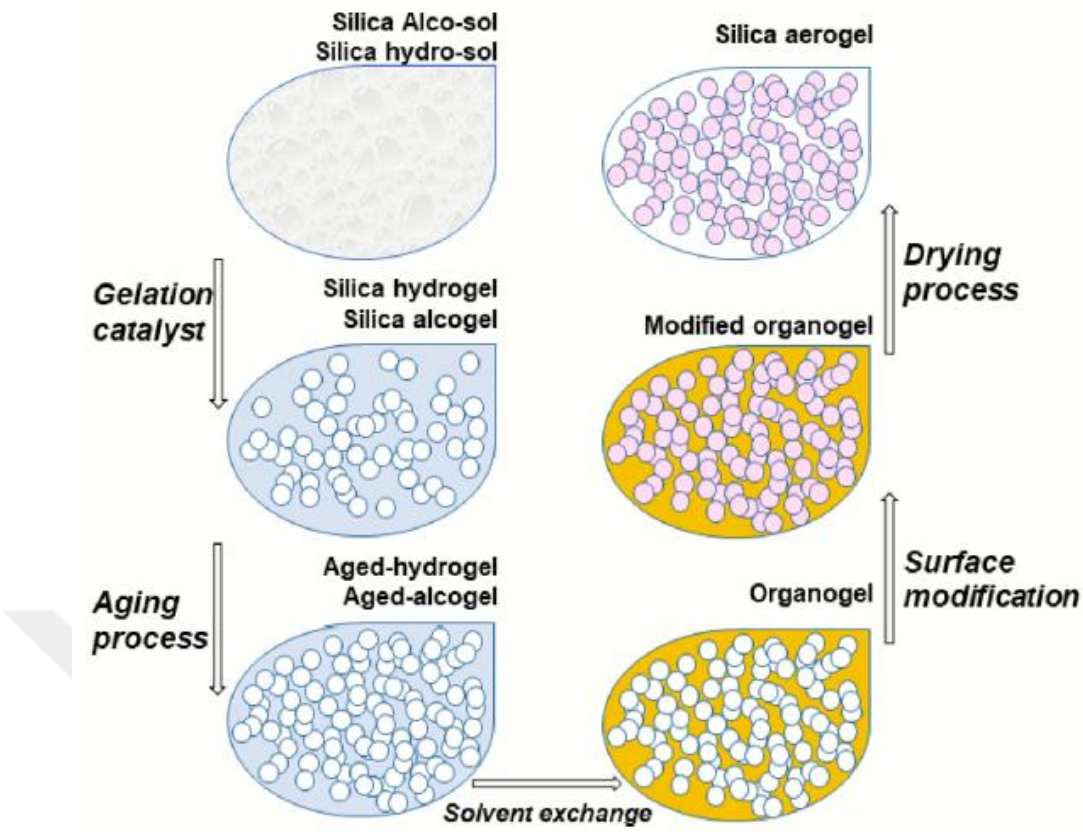

Figure 2.2: Silica aerogels synthesis. (Zahra Mazrouei-Sebdani et al., 2021).

The last stage is drying which is considered by many to be the most critical step in the synthesis process. There are different techniques in which silica aerogels can be dried with each technique resulting in a different type of aerogel with slightly different properties.

The most common drying technique is supercritical drying. This is done to avoid the high capillary during evaporation. Which if not avoided could lead to pore collapse. By using Carbon dioxide (CO_2) as the supercritical fluid based on CO_2 with its critical point at 31°C and 73 bar, is now a most common approach in industrial production despite its batch nature process. These techniques produce a solid aerogel that can be molded into different shapes and sizes and keeps the pores of the aerogel intact. It is the most porous and also the highest in terms of surface area. The Second technique is freeze-drying. This drying process produces a special type of aerogel called Cryogel. These cryogels can have pore sizes that ranges from microscale to nanoscale depending on their starting solvent, precursor concentrations, temperature and rate of freezing (Karout A et al., 2007; Guenther U et al., 2008; Kursawe M et al., 1998).

Table 2.1: The effects of aging time and temperature on the physical properties of silica aerogel (Subramaniam Iswar et al., 2017).

Aging time (hrs.)	Bulk density (g/cm^3)	BET surface area (m^2/g)	Pore size diameter (nm)	Pore volume (cm^3/g)
Aging temperature of 55 °C				
2	0.354	907	10.3	2.3
4	0.303	887	12.6	2.8
6	0.285	863	13.9	3.0
8	0.253	856	16.1	3.5
16	0.145	850	30.1	6.4
24	0.136	846	32.4	6.9
Aging temperature of 65 °C				
2	0.309	901	12.1	2.7
4	0.255	890	15.4	3.4
6	0.211	883	19.2	4.2
8	0.181	858	23.4	5.0
16	0.123	844	36.2	7.6
24	0.118	816	39.1	8.0
Aging temperature of 75 °C				
2	0.238	885	16.7	3.7
4	0.205	878	19.9	4.4
6	0.189	865	22.1	4.8
8	0.158	864	27.0	5.8
16	0.111	860	39.6	8.5
24	0.111	838	40.6	8.5

The last drying technique is ambient pressure drying which is mainly used to produce silica aerogel granulate and powder at an industrial scale. Capillary forces and shrinkage are present throughout ambient pressure drying, but with some surface modification and aging it is kept under control. This method produces what is known as Xerogel which is a type of aerogel that is denser if compared to the super critically dried aerogel as shown in Figure 2.3.

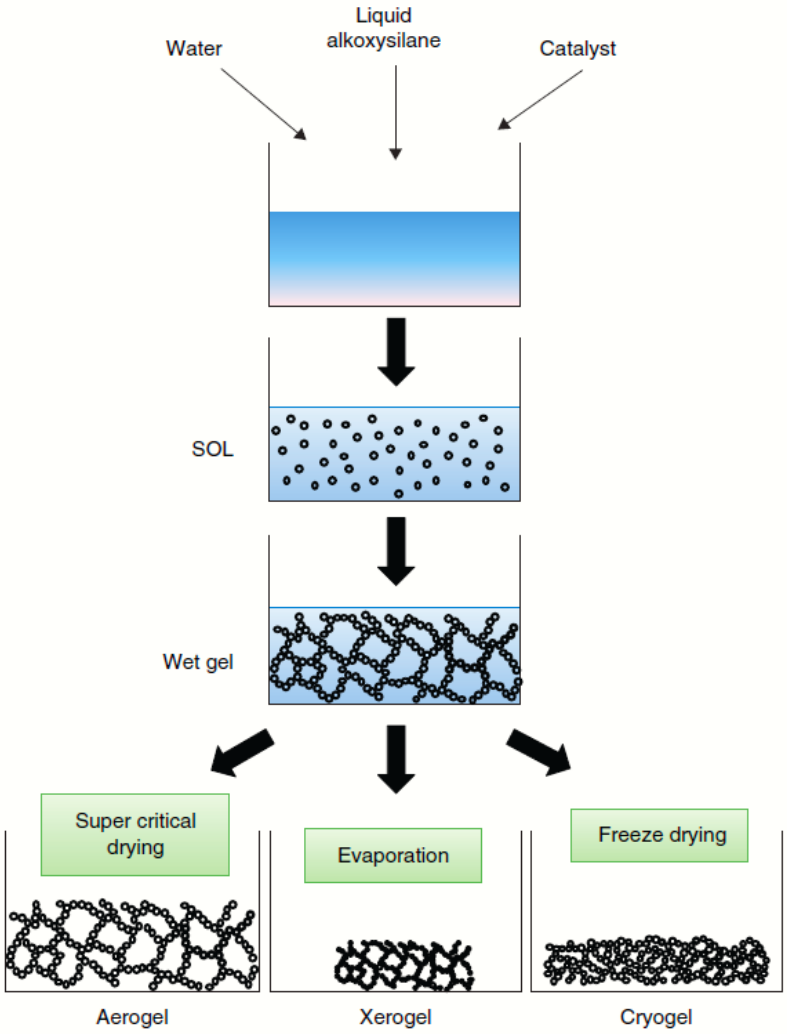

Figure 2.3: Aerogels, xerogels and cryogels synthesis (David Quintanar-Guerrero, et al., 2009).

2.1.2 Silica aerogel properties

The mechanical properties of silica aerogels are dependent on its bulk density (J.C. Wong et al., 2014). At low bulk density, silica aerogels exhibit a plastic deformation when compressed. At higher density, silica aerogels exhibit a brittle, nature despite having a higher Young's modulus than lower density silica aerogels. Furthermore, the porous and pearl like necklace structure of said aerogels confines its mechanical strength making it not suitable in cases where mechanical strength is a priority. On the other hand, this porous structure and small pore sizes enhance the performance of silica aerogels thermal conductivity performance to the point where its thermal conductivity can be less that of air.

2.1.3 Silica aerogel applications

Due to the unique properties of silica aerogels, they have been used in multiple applications some of these are;

Thermal applications which are without a doubt the most common application for silica aerogels is in thermal insulation. Applications in this field have reached full industrial scale production; from low heat transfer pipes to machines and vehicles used in space. As well as all sorts of thermal protecting clothes.

There are energy applications as well. These applications range from kinetic energy absorbing fillers to shock absorption. Although this field is yet to reach an industrial level it is still prominent in the academic field.

In addition to that it is used as well in Acoustics, catalysis as well as in biomedical applications practically as a drug carrier.

2.1.4 Xerogels

Xerogels are kind of a special form of aerogels. They are obtained when the sol-gel is dried at ambient conditions. Xerogels are porous materials like aerogels. They are made of ambient dried, cross-linked polymeric networks. They have characteristics similar to aerogels such as high porosity, high surface area, but at a less complicated and much cheaper production cost. Similar to aerogels, xerogels can be prepared from either organic or inorganic precursors. The most notable advantage of xerogels is thigh drug-loading capacity and the ability to maintain a sustained drug release. They are also biocompatible and non-toxic, making xerogels suitable for many biomedical applications. (Abdul Khalil HPS et al., 2022).

2.2 Nanofibers

Materials in the nanoscale level have been heavily contributing in many of the recent studies. Due to their variety of fabrication and adjustable wide range of properties, they have been heavily adopted in many fields; some of which are filtration, wound dressing, tissue engineering and drug delivery. Working with nanoscale eliminate many of the limitation that comes with working in microscale.

In recent years, nanofibers have taken a huge leap in the biomedical field. It has been a major contributor to advancement of drug delivery, wound dressing and tissue

engineering by taking advantage of its large surface area in improving adhesion to cells, proteins, or carrying drugs. It is also worth noting that apart from the biomedical field there are many applications of nanofibers especially in the field of filtration, fuel cells and fabric technology (Verbiˇc, A. et al., 2019; Tamura, T et al., 2010; Wang, N et al., 2014). The unique one-dimensional structure of nanofibers gives it an edge over other materials. This unique structure provides it with a large surface and a high carrying positional. Nanofibers have high mechanical bending leeway (Persano, L et al., 2011), decent optical and thermal conductivity, high electrical conductivity (Serafin, A et al.2021). and a low density (Wang, H et al., 2020) with a high aspect ratio (Zhang, W et al., 2021).

2.3 Electrospinning

There are numerous methods used for nanofiber fabrication including self-assembly, phase separation, template synthesis (Nayak R et al., 2011; Beachley V et al., 2010) and most importantly electrospinning.

Nonetheless, electrospinning is by far the most dominating method. This is due to many advantages that electrospinning has over the other methods making it very hard to compete with it especially when it comes down to 2D and 3D structure fabrication.

Electrospinning is extremely simple, affordable and relatively fast making it the most effective method to fabricate nanofibers.

A typical electrospinning apparatus consists of ahigh voltage power supply, a pumping unit to feed the solution, a syringe with a metallic tip and a surface where the nanofibers will be collected as shown in Figure 2.4.

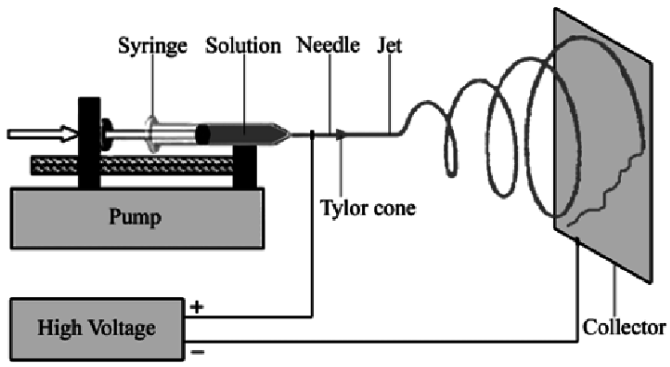

Figure 2.4: Typical electrospinning apparatus setup (Seyedin, et al., 2008).

The working concept is fairly simple, the high voltage power supply provides a high voltage to the electrospinning solution. This creates an electrical field between the metallic tip of the syringe and the collector. This electrical field works as a force to draw and stretch the electrospinning solution from the tip of the syringe to the surface of the collector where nanofibers are collected. This is done when the electrical field force overcome the surface tension of electrospinning solution. There are key parameters that affect the produced nanofibers. Some of these paraments are solution related, some are production related while others are related to the work environment in which the electrospinning process occurs. Material related parameters such as the concentration of the solution, its viscosity and molecular weight can drastically change the resulted fiber diameter therefore changing its properties. Production related parameters such as amount of voltage applied, flow rate and distance between the tip of the syringe and the collector also impact the produced fibers diameter and properties. Temperature and humidity are also important environmental factors that affect the produced nanofibers.

2.3.1 PVA electrospinning

PVA is at the top list of synthetic polymers to be ever used for biomedical applications such as artificial skin, wound healing and drug release. This is due to its biodegradable nature and its chemical and thermal stability. It also has high ability to produce fiber and high tensile strength (Hu X, et al., 2014). PVA has been a part of many composite mats fabricated by the electrospinning and it has showed that using PVA improves their spinnability mechanical properties, tensile strength, chemical and thermal stability (Yang X, et al., 2019).

2.4 Drug Delivery Systems

In order for a drug to be introduced to the body, a drug delivery system has to be utilized. This drug delivery system main goal is to be able to hold the drug, carries it to the targeted location and release it efficiently into the blood stream while limiting its potential side effects. One of the key factors in any drug delivery system is its release mechanism. There are mainly three types of drug release mechanisms. Conventional release i.e., immediate release where the release of the drug occurs immediately at a rapid pace hence the name immediate release. The second type is

sustained release which describes a slow release of the drug over a period of time. The third type is controlled release which also describes a slow release of the drug as well but at a predictable and programmed rate. Controlled release does not differ by much from sustained release. With controlled release, the drug is released over time in correlation with concentration which is not the case in sustained release. These three methods have their own merits and demerits and they are utilized depending on the drug and the targeted area. By looking at plasma concentration data of those different methods, it is apparent the difference between there release mechanism as shown in Figure 2.5.

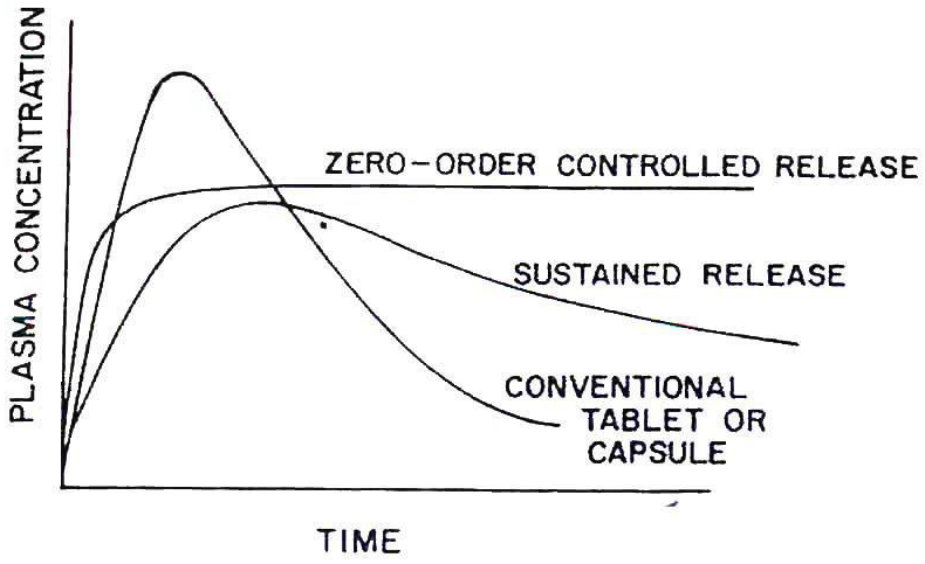

Figure 2.5: Plasma drug concertation for conventional, sustained and controlled dug release (Nautyal, U et al., 2020).

2.4.1 Aerogels in drug delivery systems

Aerogels unique properties from its high porosity to its high specific surface are what made it a very attractive material for drug delivery. As with any drug delivery system the first step is loading of the drug. Aerogels can be loaded with drugs using different techniques. The first technique is by simply adding the drug to the precursor solution during aerogel synthesis. Although this technique is simple and straightforward yet it can be limiting. Drugs used by this technique have to withstand the gelation process and the solvent exchange during the aging process otherwise the drug can be prematurely released. This limits the choices of drugs that can be loaded using this technique (C.A. García-Gonz´alez et al., 2011).

The second technique is by utilizing the solvent exchange process. After the gelation process, the gels are put into a solution of the drug. The drug will slowly seep into the pores of the gel as the solvent is leaving the pores. The main issue with this technique is it is very slow (Z. Ulker et al., 2017).

The third Technique takes advantage of the drying stage specifically aerogels dried through CO_2 supercritical drying method (M. Villegas et al., 2019; M. Salgado et al., 2017). This technique is also limited to drugs that can be dissolved in supercritical CO_2. Lastly, drug can be loaded into the aerogels after they have been dried. This is a diffusion process in which aerogels are exposed to a drug solution where the aerogel swells and drug takes place inside aerogel pores (Z. Ulker et al., 2020). although this technique adds an extra stage of production but it covers most of the drugs. Figure 2.6 shows the different techniques of drug loading in aerogels discussed above.

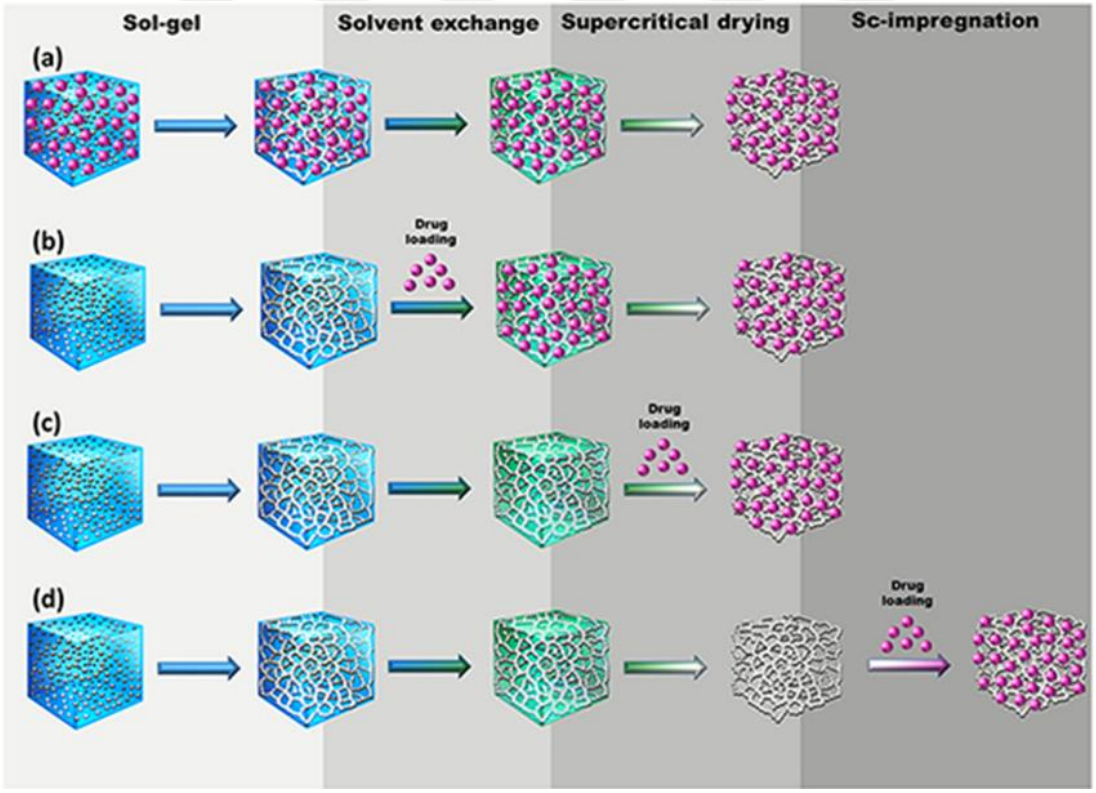

Figure 2.6: Drug loading techniques in aerogels: (a) loading during gelation; (b) loading during solvent exchange; (c) loading during drying (supercritical drying) and (d) loading through diffusion. (Carlos A. García-González et al., 2021).

2.4.1.1 Silica xerogels in drug delivery systems

Silica xerogels are an extremely attractive drug carrier option for controlled/sustained drug delivery systems. This is due its low processing temperature, improving in situ incorporation of the drug into the silica xerogel network. Xerogels are also biodegradable and possess high drug loading capabilities. The use of silica xerogels as a carrier for controlled drug delivery has been investigated since the early 1980s (T.A. Esquivel-Castro et al., 2019). There has been a wide variety of approaches to introduce drugs such as reserpine, codeine and ephedrine into silica xerogels. Majority of these approaches where in tablets or capsules form (S. Saeed et al., 2015). There are three synthesis factors that affects silica xerogel drug carrying performance. These factors can be shown in Table 2.2.

Table 2.2: Synthesis factors that affects silica xerogel drug carrying performance.

Synthesis factor	Effects
Water/alkoxide ratio	The less water used during synthesis, the more porous and linear the structure contrary to using a large amount of water which would result in a branched structure
Temperature	The higher the temperature of drying the more the pores of xerogel are compressed
Catalyst	Catalyst of a basic nature results in a branched structure while acidic catalyst results in a more linear structure

2.4.2 Nanofibers in drug delivery systems

Nanofibers extraordinary properties such as high surface area and high porosity are very desirable properties for drug delivery systems. Electrospinning is a fabrication method generally used to fabricate a drug loaded nonfibrous mat.

There are different strategies that can be used to fabricate a nanofibrous mat loaded with drug. In the first strategy, a polymer solution is prepared, and then drug is mixed into this polymeric solution. This is later electrospun to fabricate nanofibrous mat loaded with drug (Fernández de la Mora, J., 2007). The second strategy is done by adding drug carriers to the polymeric solution and then electro spin it. The drug carriers hold the drug and are attached to outside of the nanofibrous mat, another strategy is to have the drug added to the nanofibrous mat after it has been electrospun. Lastly, by

utilizing Core-shell electrospinning; drug can work as the core with the nanofibers working as the shell covering it. These different strategies can be shown in Figure 2.7.

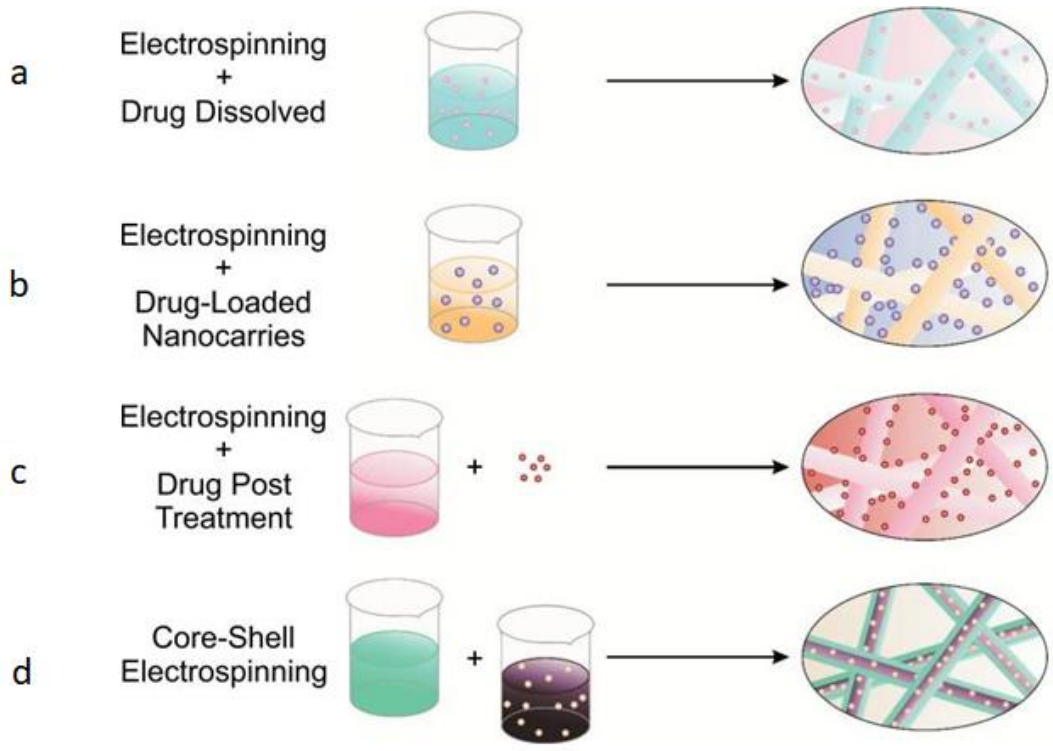

Figure 2.7: Different strategies used to fabricate drug loaded nanofibers. (a) Drug dissolved into polymeric solution (b) Drug is carrier by drug carriers mixed in the solution. (c) Drug is added after electrospinning. (d) Core-shell electrospinning utilization. (Fernández de la Mora, J., 2007).

2.5 Topical Drug Delivery Systems

The concept of delivering drugs to and through the skin has always been attractive for many reasons. Perhaps the most important one is it avoids the drug passing into the liver first which would limit many of the side effects of the traditional oral way of drug delivery and increase the effectiveness of the drug carried. Obviously, this does not replace oral drug delivery as with some drug and diseases topical drug delivery is just not an option. Topical drug delivery also helps treat local infections and inflammations and even some skin tumors that are not easily accessible by the means of traditional drug delivery systems. It also offers the flexibility to stop and cut the treatment at any point of time which is something that systematic systems lack.

2.6 Steroids

Steroids, also known as corticosteroids, are anti-inflammatory medicines used to treat a wide range of conditions such as asthma, eczema and arthritis. In a study done by Sieminska et al. a slow-release drug delivery system using silica xerogel loaded with four different steroids were prepared. These steroids were progesterone, estradiol, estrone and hydrocortisone. These steroids were incorporated into the silica xerogel by means of soaking them in steroid/benzene or ethanol solution. In his study, Sieminska et al. concluded that diffusion of steroids in silica xerogel was determined by many parameters, such as the carrier solvent, silica xerogel pore size diameter and the size of the drug molecules (Sieminska L et al.,1997).

2.6.1 Hydrocortisone

steroids used in Sieminska et al. study were successfully incorporated into the silica xerogel during synthesis with hydrocortisone being the only exception. Hydrocortisone loaded during the synthesis of the silica xerogel resulted to it being permanently trapped inside the silica xerogel pores rendering this loading strategy unusable when attempting to produce a silica xerogel carrying hydrocortisone. On the other hand, introducing hydrocortisone to the silica xerogel after the synthesis proved to be the most suitable strategy for loading silica xerogel with hydrocortisone.

3. EXPERIMENTAL WORK

3.1 Materials

3.1.1 Xerogel synthesis

Tetramethyl orthosilicate (TMOS) (≥99%) as the silica precursor, Methanol (≥99.8 % Gas chromatography (GC)), Ammonium hydroxide (NH_4OH) to work as a solvent, 28-30 wt % in water were purchased from Sigma Aldrich (USA).

3.1.2 Nanofibers fabrication

PVA (average molecular weight= 146,000 – 186,000) was purchased from Sigma Aldrich (USA). Distilled water was made available by Milli-Q Ultrapure Water System. All chemical solvents used at analytical grade and with no purifications.

3.1.3 In vitro analysis studies

Ethanol (≥99.8 % GC), Phosphate buffer saline 7.4 (PBS) And Hydrocortisone were purchased from Sigma Aldrich (USA). Dialysis tubing cellulose membrane (average flat width 34 mm), consisting of regenerated cellulose, was purchased from Genesuz (Turkey).

3.2 Methods

3.2.1 Xerogel synthesis

TMOS is the silica precursor. TMOS is hydrolyzed by water so that it can polymerize. Methanol works as a co-solvent because it is miscible with both TMOS and water which helps bringing both into the same phase so they can react with each other's. Ammonium hydroxide works as an alkaline catalyst helping to make the reactions go faster.

In order to keep the synthesis process simple and streamlined, three solutions were prepared. Firstly, NH_4OH stock solution was prepared by adding 4.86 g (5.40 mL) of

concentrated NH_4OH to 1000 mL of distilled water. Secondly, an alkoxide solution was prepared by mixing 2.04 g (2.0 mL) of the silica precursor TMOS and 1.58 g (2.0 mL) of methanol. The last solution was the catalyst solution which was prepared by mixing 5.0 g (5.0 mL) NH_4OH stock solution that was prepared earlier with 1.58 g (2.0 mL) of methanol. Lastly, by mixing the catalyst solution with the alkoxide solution for 1-2 min a sol-gel solution was obtained as shown in Figure 3.1.

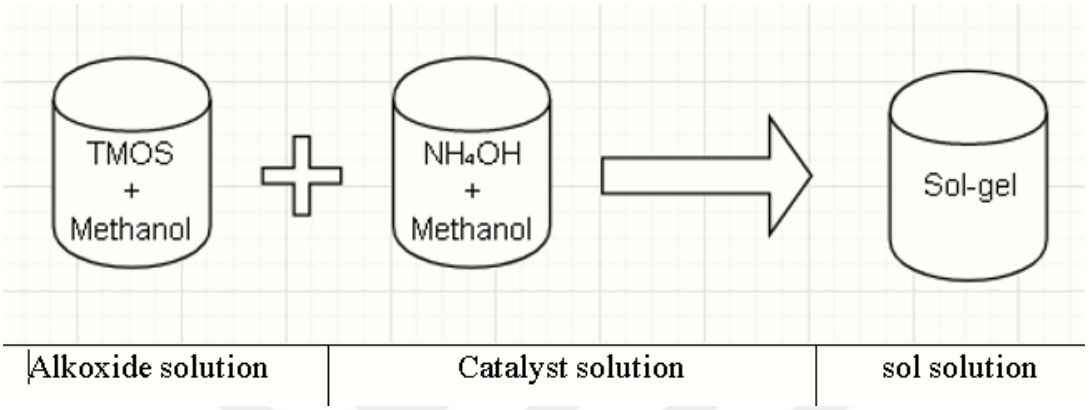

Figure 3.1: Xerogel synthesis.

This sol-gel solution was then poured into small cylindrical molds of around 1.5 cm in diameter and 3 cm in height. The sol-gel solution was left in the molds to fully solidify.

After completely solidifying, the produced silica xerogel samples were left to age in methanol for around 5 days with replacing old methanol with fresh one every 24 hours. After that samples were dried at ambient temperature and the results are shown in Figure 3.2 below.

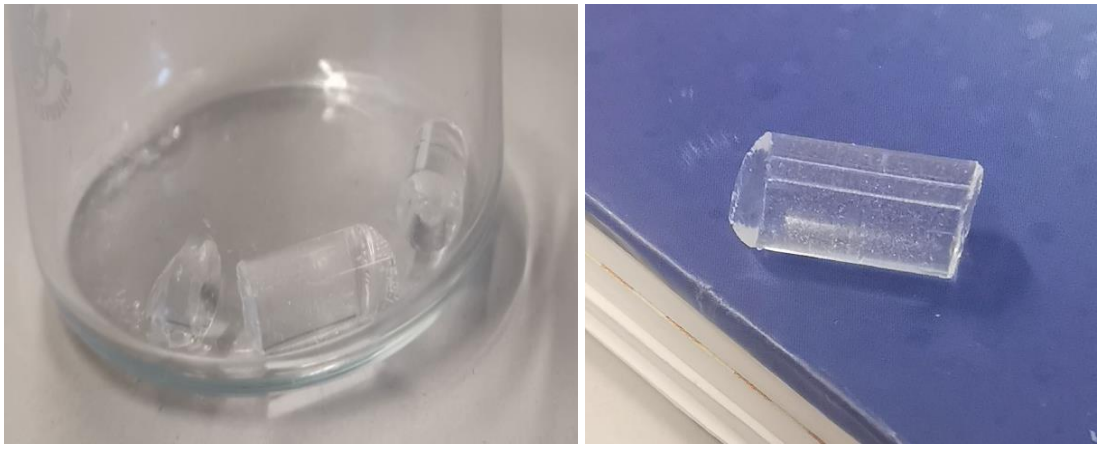

Figure 3.2: Synthesized xerogel.

3.2.2 Ball-milling

The working principle of mechanical ball milling is simply the utilization of high energy to grind down and reduce the particle size of a material. This process results in particles size reduction ranging from micro sized particles to even nanosized ones depending on the material being milled, frequency and time of the process (Janani Balasubramanian et al,.2022). There are different types of ball miller with different milling techniques such as vibrating ball mills, high energy mills and low energy mills, (Janani Balasubramanian et al,.2022).

To start the size reduction process, samples of the silica xerogel are put into a container containing 4 different sizes of heavy balls. This set of balls help with size reduction of the xerogel samples by continuously grinding against them. The ball-milling process was done at a frequency of 30hz for around 15-20 minutes using SFM-1 desk planetary ball miller shown in Figure 3.3. and the results were a fine xerogel powder as shown in Figure 3.4.

Figure 3.3: SFM-1 desk planetary ball miller.

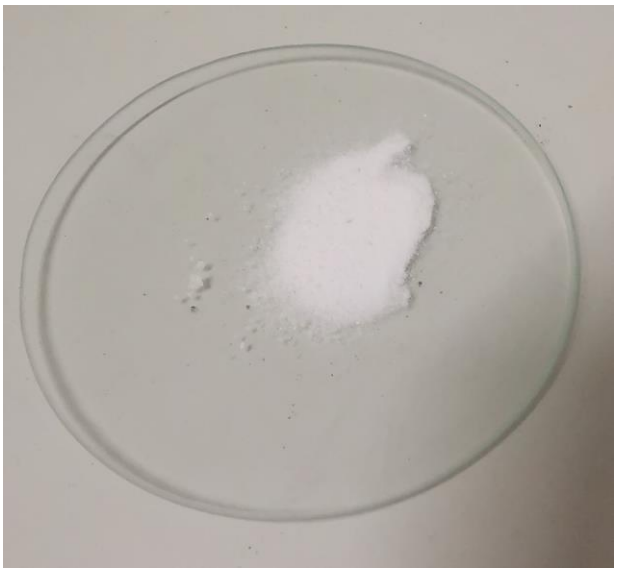

Figure 3.4: Ball-milled silica xerogel.

3.2.3 Drug loading

Hydrocortisone was opted to be used as the drug in this study. There were two options to load the drug into the silica xerogel. The first option is by adding the drug during the synthesis process which would reduce production time but it may result in hydrocortisone being trapped inside the silica xerogel permanently (Sieminska L et al.,1997). The second option was to add the hydrocortisone after the synthesis process. This would add another step into production but it ensures no reaction or change happing to the hydrocortisone during the loading process which was the approach taken here. Aiming at a ratio of 1:2 Hydrocortisone to silica xerogel a solution consisting of 1% Hydrocortisone-ethanol was prepared using about 25mg of hydrocortisone. Then about 50 mg of the ball-milled silica xerogel powder was added to the drug solution. The solution was kept at ambient temperature for 5 days. Lastly, the drug loaded silica xerogel was filtered and dried at ambient condition.

3.2.4 Preparation of the electrospinning solutions

Silica xerogel loaded with hydrocortisone cannot be electrospun on their own due to the inherit weakness of the xerogel structure. Therefore, PVA was used as a supporting polymer. The solvent used was distilled water. 6%, 8% and 10% of PVA solutions were prepared by adding the proper amount of PVA into distilled water and stirring it for 3-4 hours at around 90 °C.

3.2.4.1 Preparation of the PVA/hydrocortisone solutions

An amount of 5 mg of hydrocortisone was added to each of the three different concentrations of PVA solutions. The solutions were stirred for 3 hours at ambient temperature. This is for use as a control to the PVA/xerogel/hydrocortisone.

3.2.4.2 Preparation of the PVA/xerogel/hydrocortisone solutions

An amount of 10 mg of the ball-milled silica xerogel loaded with hydrocortisone was added to each of the PVA solutions. These solutions were also stirred for 3 hours at ambient temperature.

3.2.5 Nanofibers fabrication

The process of nanofibers fabrication was done using a typical needle electrospinning setup with a horizontally oscillating collector as shown in Figure 3.5. All electrospinning trials were done under ambient conditions. electrospinning device used for nanofibers fabrication.

Figure 3. 5: Electrospinning apparatus used in the study.

3.2.5.1 Fabrication of PVA/hydrocortisone

The three solutions of 6%, 8% and 10% PVA loaded with hydrocortisone were prepared for electrospinning. Both the 10% and 8% PVA loaded with hydrocortisone solutions were not able to be spun and kept clogging the needle and barely managed to produce any fibers. On the other hand, the 6% PVA loaded with hydrocortisone was able to be electrospun smoothly with little to no problems at all. The electrospinning parameters used during this process are shown in Table 3.1.

Table 3.1: Electrospinning parameters.

Parameter	Value
Flow rate	1.0 mL/hr.
Voltage	20kV
Distance	15 cm

3.2.5.2 Fabrication of PVA/xerogel/hydrocortisone

Expectedly, Both the 10% and 8% PVA/xerogel/hydrocortisone solutions had the same problem with electrospinning and did not produce any fibers. The 6% PVA/xerogel/hydrocortisone was able to be electrospun with ease. The electrospinning parameters used during this process were kept the same as the control samples parameters shown in Table 3.1 above.

3.2.6 UV-Vis absorbance study

Ultraviolet–visible (UV-Vis) spectroscopy is an analytical method used to measures the number of discrete wavelengths of UV or visible light that are absorbed by a sample and comparing it to a blank sample (Figure 3.6). UV-Vis spectroscopy relies on the use of light Therefore, it is highly dependent on the properties of light itself. The amount of energy a light can carry depends on its wavelength. The shorter it is the more energy it can carry and vice versa. Depending on substance used the energy required for absorbance changes this is why light absorption happens at a different wavelength for different substances (Gersing S, Cagiada M, Gebbia M, et al., 2023).

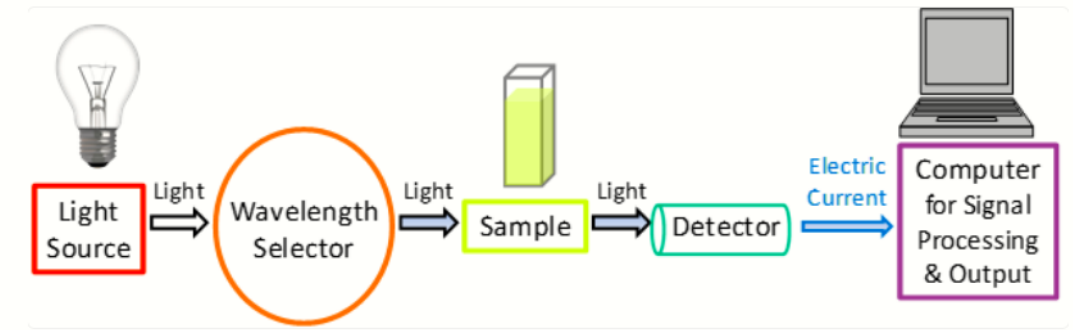

Figure 3.6: Schematic of a UV-Vis spectrophotometer (Gersing S, Cagiada M, Gebbia M, et al., 2023).

UV-Visible 2600 Shimadzu spectrophotometer (Figure 3.7) was used to determine the amount of UV radiation that is absorbed by the drug in the solution. This is simply done in accordance to Beer-Lambert law.

Equation 3.1 expresses Beer-Lambert law which describes the linear relationship between the absorbance of electromagnetic radiation and concentration.

$$A = \varepsilon cL \tag{3.1}$$

where;

A is absorbance

L is optical path length

c is concentration of solution

ε is molar extinction coefficient.

Equation 3.2 shows the mathematical relationships between Beer–Lambert's law, the light intensity and transmittance (Picollo, et al., 2019; Sharpe, M. 1984).

$$A = \varepsilon cL = \log_{10}(I_0 / I) = \log_{10}(1/T) = -\log_{10}(T) \tag{3.2}$$

where;

I_0 is incident intensity

I is transmitted intensity

T is transmittance.

Figure 3.7: UV-Vis spectrometer used in this study.

3.2.6.1 Calibration curve

In order to determine the cumulative hydrocortisone release percentage of the silica xerogel carrier a calibration curve was plotted. This was done by dissolving 5 mg of hydrocortisone in 10 mL of PBS to be used as a stock solution. The stock solution was then diluted to different concentrations of 5, 10, 20, 30, 40, 50, 60, 70, 80 and 90 µg/mL using serial dilution. All of these solutions were tested at a wavelength range of 200 to 400 nm by the UV-Vis spectrometer with a peak of 280 nm. The data required were analyzed and a calibration curve was plotted describing the relation between the concentration to the absorbance. The slope and coefficient of determination (R^2) were calculated as well.

3.2.6.2 In Virto drug release study

Firstly, silica xerogel powder loaded with hydrocortisone was placed inside a dialysis tubing made of regenerated cellulose. The dialysis tubing was then sealed from both ends and suspended in a flask containing 100mL of PBS. Making sure that the sample was fully submerged in the buffer solution, the flask was then sealed and covered to avoid light passing through and affecting the results as shown in the Figure 3.8.

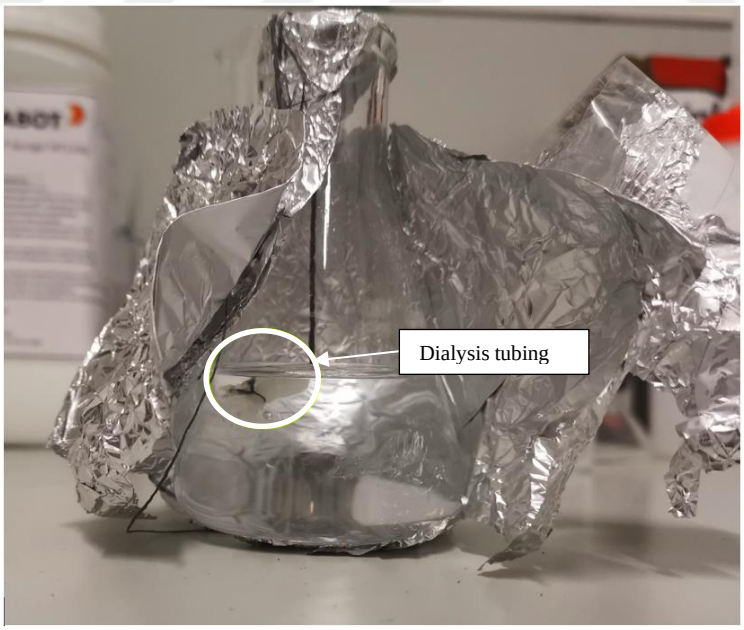

Figure 3.8: Silica xerogel loaded with hydrocortisone inside the dialysis tubing suspended in the PBS.

Secondly, the solution was stirred at 100 rpm at a temperature of 37°C. At exactly at 1, 2, 4, 8, 16 and 25 days a sample of 2 mL was taken from the solution for testing and

2 mL of fresh PBS was added into the solution. Each sample was then scanned by UV-Vis spectrometer at wavelength 280 nm. Using the calibration curve plotted earlier, the hydrocortisone concentration in the solution was determined and cumulative release percentage was calculated. Furthermore, a graph conveying the change of hydrocortisone cumulative release percentage across time in days was plotted.

Thirdly, a 20mm in diameter circle shaped sample of the PVA/xerogel/hydrocortisone solution was cut and placed inside a dialysis tubing as well in order to recreate the same experiment mentioned above. Samples of 2 mL were also taken at 1, 2, 4, 8, 16 and 25 days for testing and 2 mL of fresh PBS was added into the solution. These samples were also scanned by UV-Vis spectrometer at same wavelength of 280 nm. The data acquired have been analyzed to observe the change of release behavior of the hydrocortisone inside the electrospun mat.

Lastly, a 20mm in diameter circle shaped sample of the PVA loaded with hydrocortisone was cut and placed inside a dialysis tubing. The sample was subjected to the same experiment with the only exception being the time intervals at which samples from the solution were taken for testing. The new time intervals were at 15, 30, 60, 120 and 240 minutes.

3.3 Characterization

3.3.1 Surface area, pore volume and size analysis

Brunauer-Emmett-Teller (BET) surface area analysis evaluate the specific surface area of the synthesized xerogel. This is done by using nitrogen multilayer adsorption measured as a function of relative pressure. This technique involves external area and pore area valuations to determine the total specific surface area in m^2/g.

Barrett-Joyner-Halenda (BJH) analysis can also be employed to determine pore area and specific pore volume using adsorption and desorption techniques. This technique characterizes pore size distribution independent of external area due to particle size of the sample

The synthesized xerogel has been tested for BET surface area analysis and BJH pore size and volume analysis.

3.3.2 SEM/EDAX analysis

In order to perform Scanning Electron Microscopy (SEM) analysis, samples were cut into squares of 1 by 1 cm, mounted on a stub with a double-sided carbon tape and placed into a Quorum Sputter Coater as shown in Figure 3.9b to be coated with a thin layer of Gold/Palladium (Au/Pd) for 2 min. after that, a Tescan Vega3 scanning electron microscope as shown in Figure 3.9a was used to examine the electrospun samples.

Energy-dispersive X-ray spectroscopy (EDAX) was performed as well to pinpoint the different elements present in the samples.

(a) (b)

Figure 3.9: (a) Quorum Sputter Coater (b) SEM.

3.3.3 FTIR analysis

Fourier Transform Infrared Spectroscopy (FTIR) were performed for synthesized silica xerogel, hydrocortisone, PVA/hydrocortisone and PVA/xerogel/hydrocortisone samples. FTIR analysis works by measuring the range of wavelengths in the infrared region that are absorbed by the sample. This is done by applying an infrared radiation to the sample. Each sample absorb the infrared light's energy at different wavelengths which helps to determine that said sample molecular composition.

Figure 3. 10: FTIR spectrometer used in the study.

Samples were cut into small squares of around 1 by 1 cm and placed in the spectrometer shown in Figure 3.10. Force applied was 70 Newton force after the signal has been decoded, using Fourier transformation a graph was created for each sample.

4. RESULTS AND DISCUSSION

4.1 Surface area, pore volume and size analysis

Surface area, pore size and volume are crucial factors that affect the xerogel drug carrying and releasing performance. Therefore, those properties were thoroughly investigated for the synthesized ball-milled xerogel powder and compared to literature.

4.1.1 Surface area analysis

This was done to the synthesized xerogel and the result were as following:

Table 4.1: Surface area analysis summary.

Analysis	Results (m^2/g)
Single point surface area	489.0177
BET surface area	505.1433
Langmuir Surface Area	1,286.9949
t-Plot external surface area	515.1752
BJH Adsorption cumulative surface area of pores between 1,7000 nm and 300,0000 nm width	474.9243
BJH Desorption cumulative surface area of pores between 1,7000 nm and 300,0000 nm width	592.4879
D-H Adsorption cumulative surface area of pores between 1,7000 nm and 300,0000 nm width	466.5315
D-H Desorption cumulative surface area of pores between 1,7000 nm and 300,0000 nm width	564.3050

The specific surface area of xerogels varies in literature depending on many factors such as the type of catalysis used, gelation time (Arenas et al., 2007). It could be as low as 300 m^2/g and as high 900 m^2/g. Sieminska L et al., in their attempt to test diffusion of steroids in xerogels synthesized a xerogel that is capable of carrying different types of steroids such as progesterone and estradiol. The surface area of that xerogel was around 550 m^2/g.

The results shown in Table 4.1 shows that BET surface area for the synthesized xerogel is 505 m^2/g which is in line with the literature.

4.1.2 Pore volume analysis

This was done to the synthesized xerogel and the result were as shown in Table 4.2 below:

Table 4.2: Pore volume analysis summary.

Analysis	Results (cm^3/g)
Single point adsorption total pore volume of pores less than 41,9873 nm width	0.480232
Single point desorption total pore volume of pores less than 40,3122 nm	0.480995
t-Plot micropore volume	-0.011513
BJH Adsorption cumulative volume of pores between 1,7000 nm and 300,0000 nm width	0.457467
BJH Desorption cumulative volume of pores between 1,7000 nm and 300,0000 nm width	0.513395
D-H Adsorption cumulative volume of pores between 1,7000 nm and 300,0000 nm width	0.450601
D-H Desorption cumulative volume of pores between 1,7000 nm and 300,0000 nm width	0.487348

Similar to surface area, pore volume of silica xerogels varies in literature as well. The results shown in Table 4.2 shows that average pore volume for the synthesized xerogel is 0.48 cm^3/g which is in line with the literature as well (Sieminska L et al.,1997). Figure 4.1 describes the relation between pore volume and pore width. As the pore volume of silica xerogel increases the pore width increases as well. Theoretically, wider pores could carry more of the drug but it would also increase the rate at which it would release it.

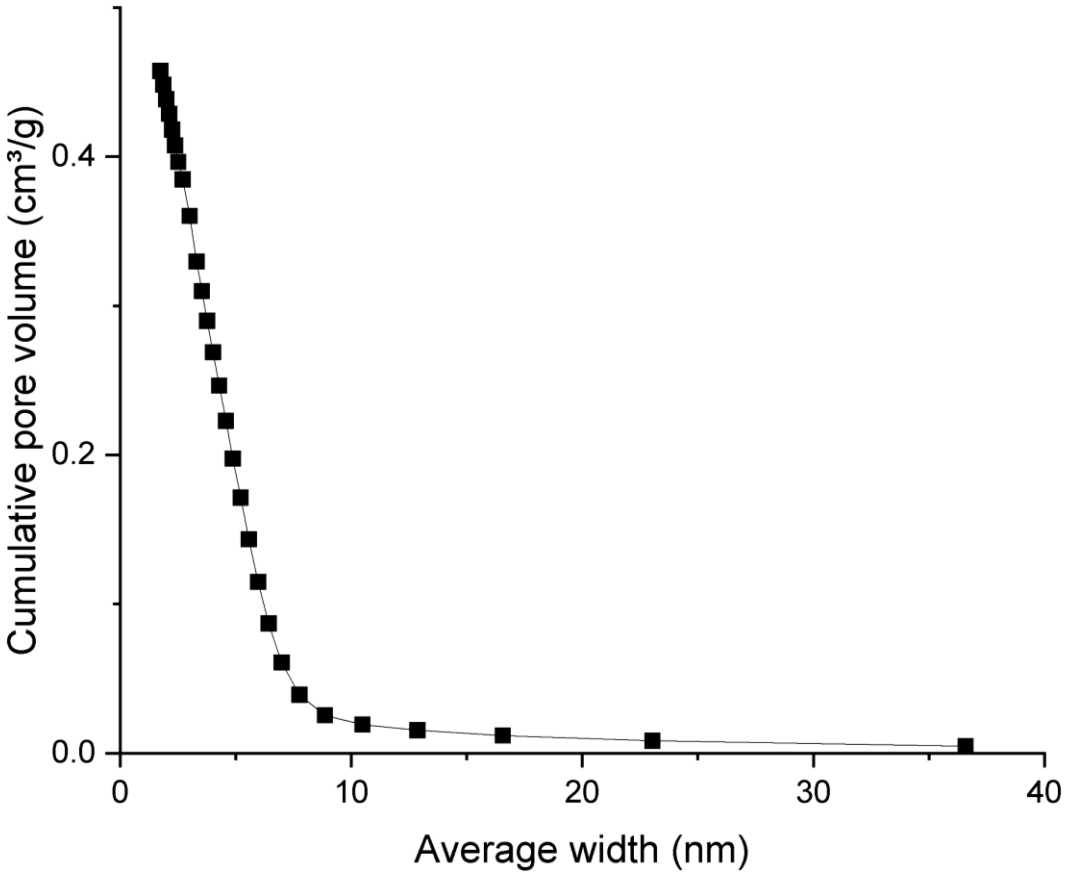

Figure 4.1: The relation between pore volume and pore width.

4.1.3 Pore size analysis

Pore size analysis was done to the synthesized xerogel and the result were as following:

Table 4.3: Pore size analysis summary.

Analysis	Results (nm)
BET Adsorption average pore diameter	3.8027
BET Desorption average pore diameter	3.8088
BJH Adsorption average pore width	3.8530
BJH Desorption average pore width	3.4660
D-H Adsorption average pore width	3.8634
D-H Desorption average pore width	3.4545

Table 4.3 above shows the average pore size of the synthesized silica xerogel. From the data we have the average pore size is around 3.8 nm. Furthermore, the average particle size of the synthesized silica xerogel was investigated as well as the median pore width and the results were as follows:

Nanoparticle Size: Average Particle Size 11.8778 nm.

Median pore width: 0.6824 nm.

4.2 SEM/EDAX analysis

SEM analysis was done to analyze the surface of the fibers and the silica xerogel within the fibers. Figure 4.2 shows the silica xerogel loaded with hydrocortisone within the electrospun PVA fibers.

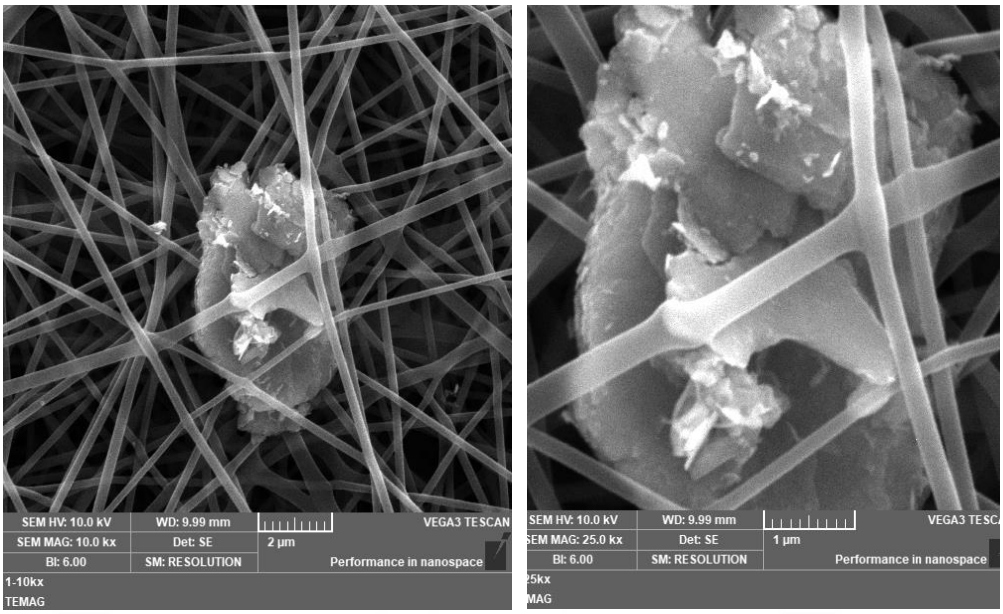

(a) (b)

Figure 4.2 : (a) Silica xerogel loaded with hydrocortisone within PVA fibers (10kx) (b) Silica xerogel loaded with hydrocortisone within PVA fibers(25kx).

EDAX was used to analyze the elements within the PVA/xerogel/hydrocortisone as well as the PVA/hydrocortisone sample. A spot was chosen randomly as shown in Figure 4.3 and element analysis was performed.

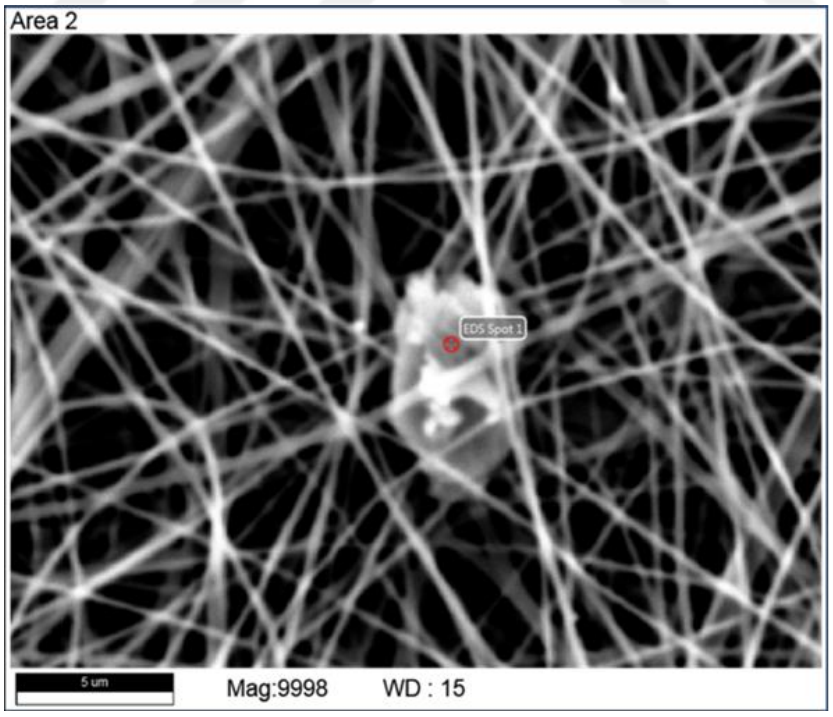

Figure 4.3: Spot were the EDAX analysis were made for PVA/xerogel/hydrocortisone.

EDAX analysis showed the existence of different types of elements as shown in Table 4.4. One of those elements is Silicone (Si) at around 18% which means that the process of electrospinning PVA with hydrocortisone loaded xerogel has been done successfully. Element such as Oxygen (O) making up a significant percentage of the weight percentage as shown in figure 4.4 is due to the existence of all of PVA, xerogel and hydrocortisone. While Aluminum (Al) element is there likely as a result to aluminum foil used to collect the fibers in the electrospinning process.

Table 4.4: EDAX element report.

Element	Weight (%)	Atomic (%)	Error (%)
C	14.30	14.30	9.80
O	48.00	48.00	6.50
Al	14.60	14.60	3.80
Si	18.00	18.00	3.80
Au	2.70	2.70	13.90
Pd	2.40	2.40	14.70

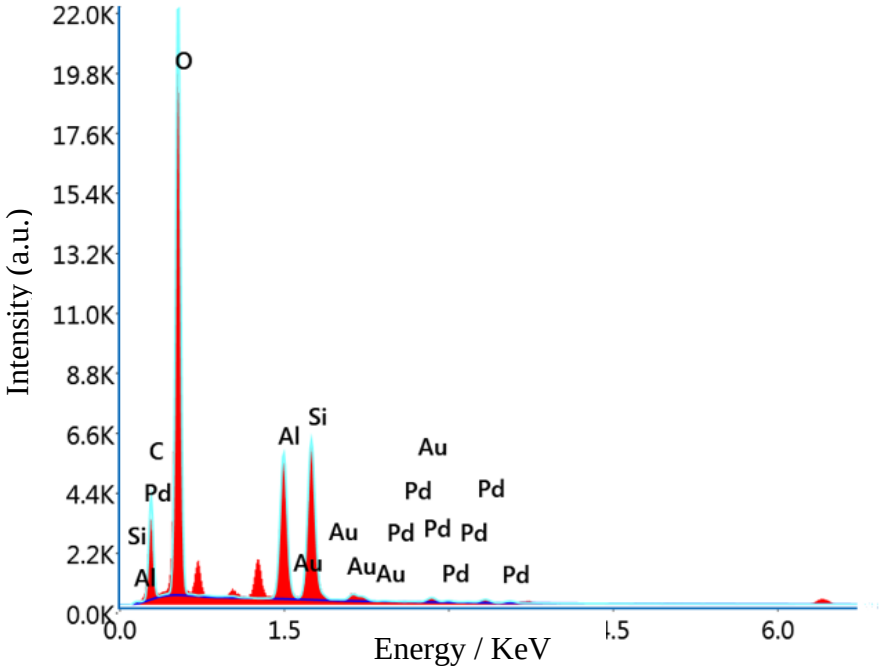

Figure 4.4: Different elements found in the EDAX spot for PVA/xerogel/hydrocortisone.

SEM analysis was also done to the PVA/hydrocortisone sample and the result is shown in Figure 4.5 below.

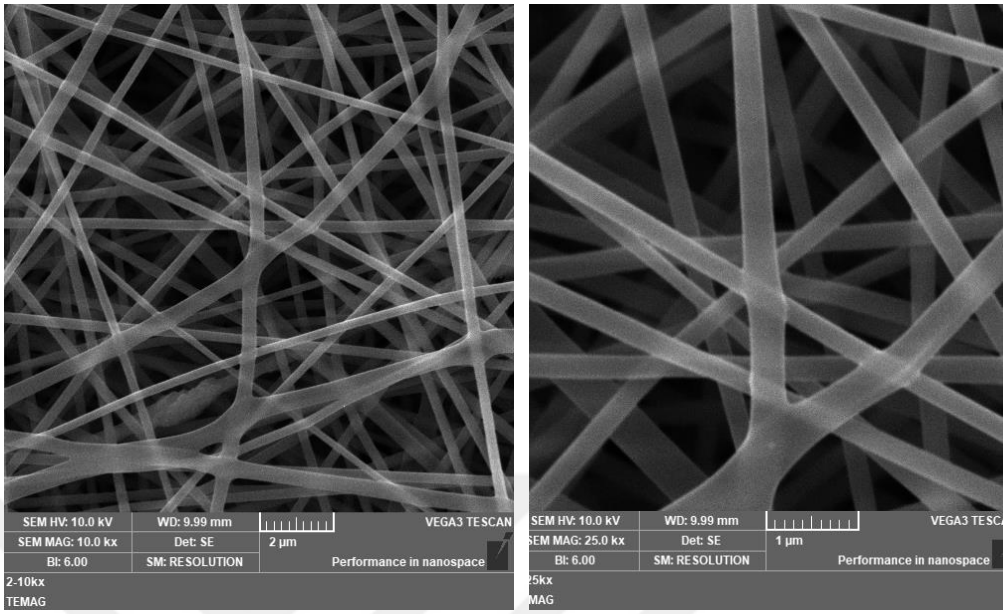

(a) **(b)**

Figure 4.5: (a) PVA/hydrocortisone (10kx) (b) PVA/hydrocortisone (25kx).

The SEM images shows no clear signs of the existence or the nonexistence of the hydrocortisone within the PVA fibers. Furthermore, EDAX analysis was performed with one spot chosen randomly as shown in Figure 4.6

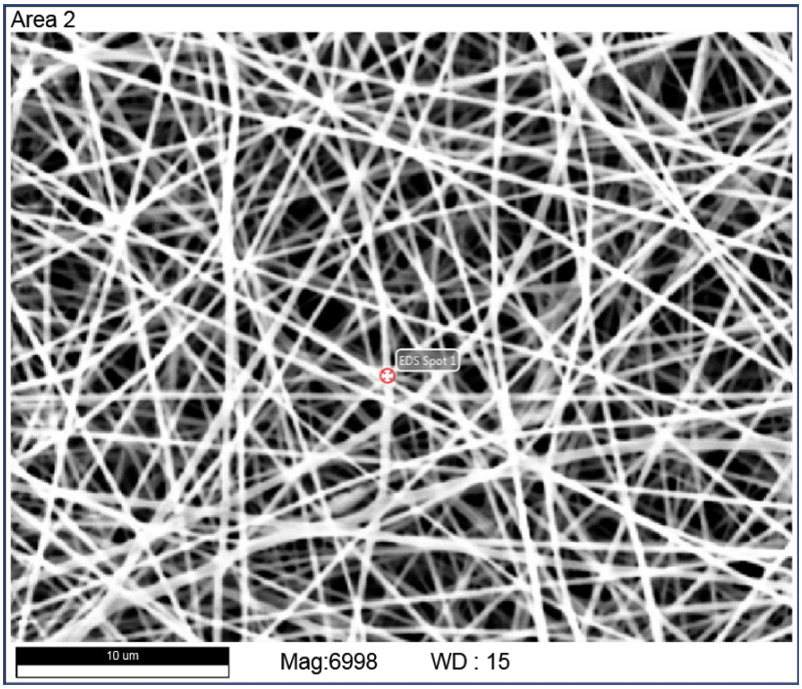

Figure 4.6: Spot were the EDAX analysis were made for PVA/hydrocortisone.

Table 4.5: EDAX spot element report.

Element	Weight (%)	Atomic (%)	Error (%)
C	63.20	79.90	4.50
O	18.80	17.80	10.80
Al	0.40	0.20	20.40
Si	0.30	0.20	28.60
Au	9.50	0.70	9.00
Pd	7.80	1.10	12.90

Table 4.5 shows a high percentage of 63% Carbon (C). This could be a sign of hydrocortisone being precent in the fibers but it is not conclusive information. There is also a decrease in Oxygen percentage compared to the PVA/xerogel/hydrocortisone sample due to the absence of xerogel. The existence of silicone element as shown in The Figure 4.7 is an anomaly as it has quite a high error percentage and it is most likely due a sample contamination.

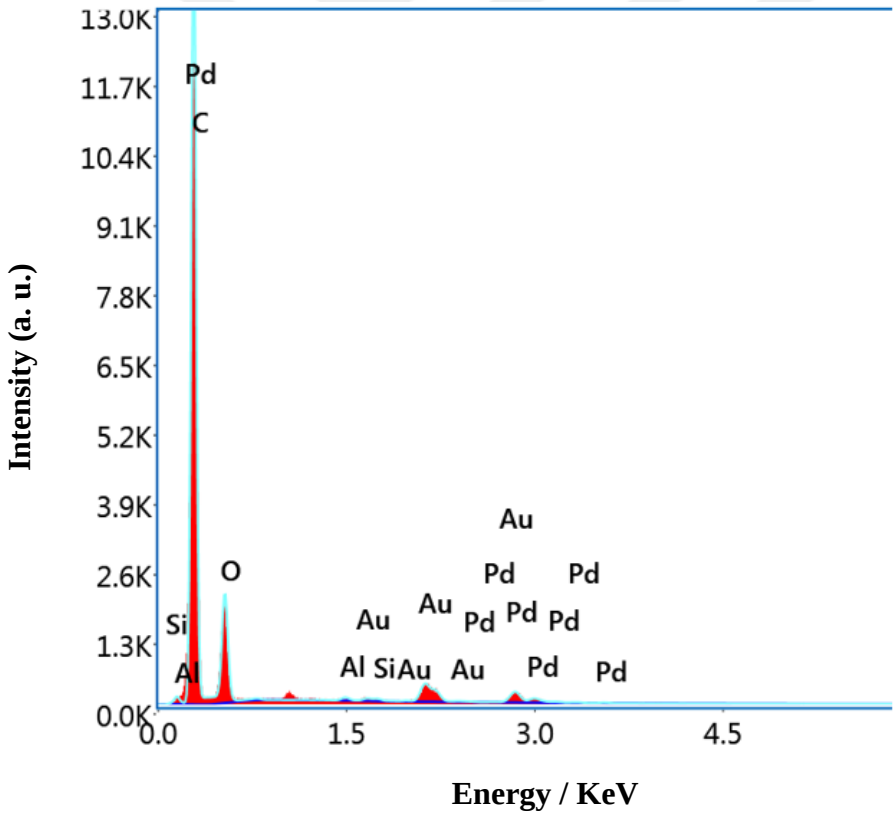

Figure 4.7: Different elements found in the EDAX spot for PVA/xerogel/hydrocortisone.

As mentioned before these results unlike the PVA/xerogel/hydrocortisone sample are not conclusive to whether hydrocortisone present in the PVA/hydrocortisone sample or not. Therefore, FTIR analysis had to be performed to have conclusive information.

4.3 FTIR Analysis

4.3.1 Silica xerogel analysis

After the process of synthesizing the silica xerogel and ball milling it, the produced silica xerogel powder was analyzed with FTIR and results were compared with literature as shown in both Figure 4.8 and 4.9.

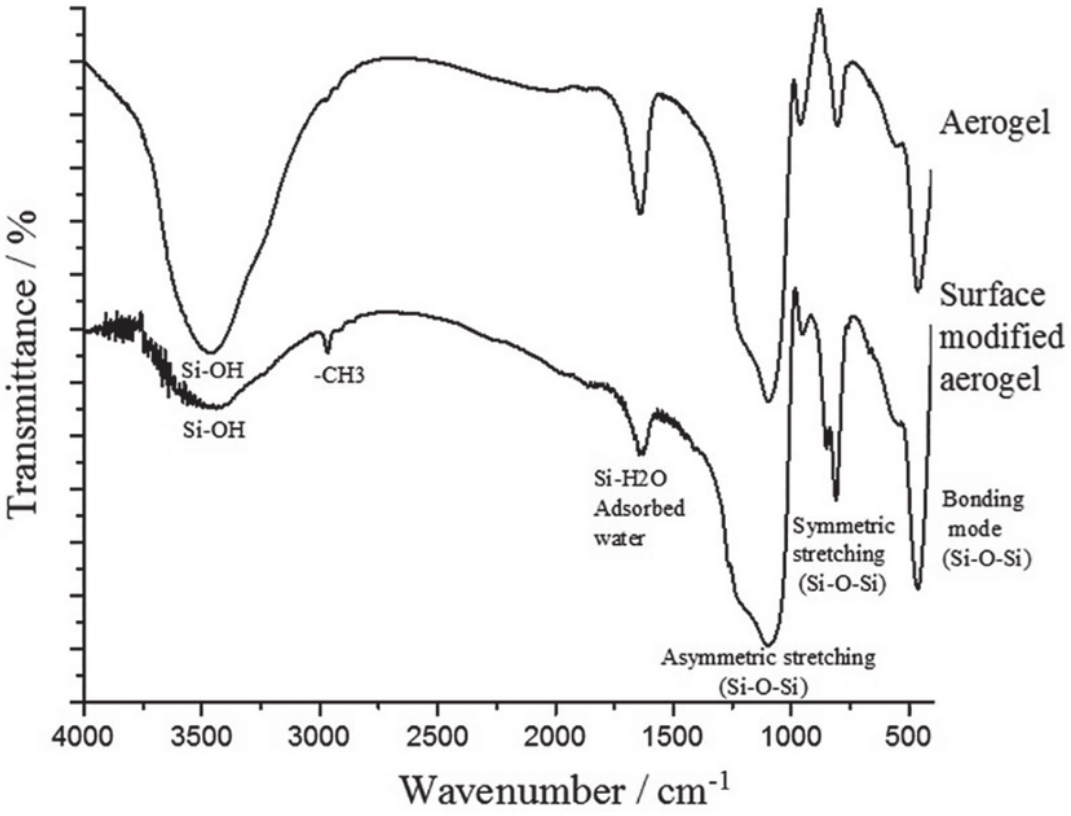

Figure 4.8: FTIR spectra of the silica aerogel nanoparticles before and after surface modification. (Nguyen et al., 2018).

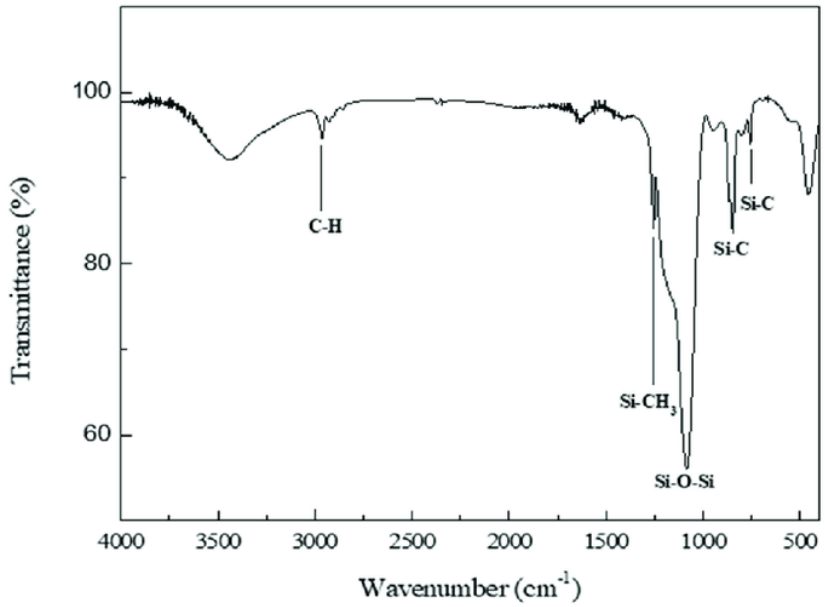

Figure 4.9: FTIR spectrum of the surface-modified silica aerogel. (Ban et al., 2019).

In this study, no surface modification has been done to the synthesized silica xerogel. The resulted xerogel was identical to the ones shown in various literature sources with the exception of the absence of the Si-C peaks due to lack of surface modification as shown in the Figure 4.10.

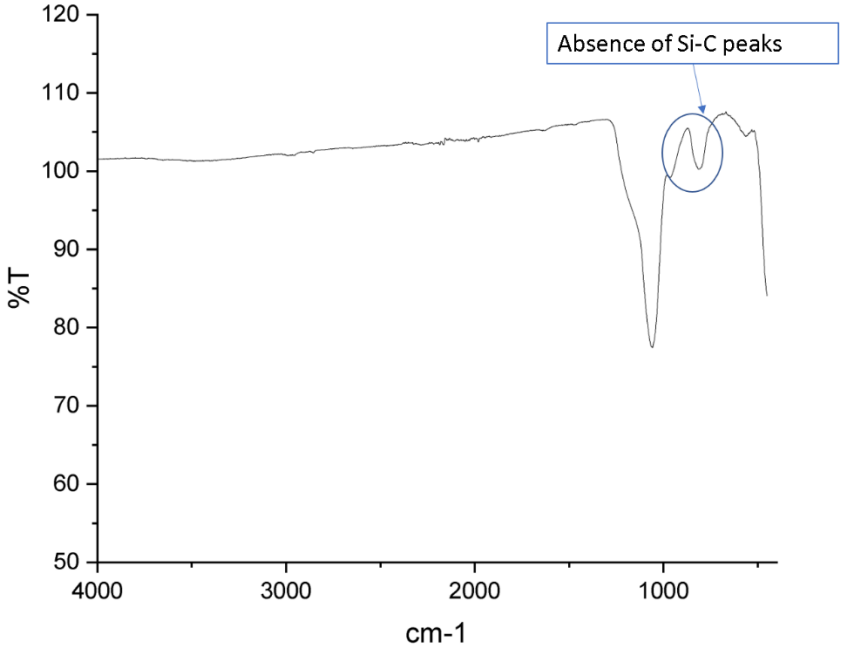

Figure 4.10: FTIR spectrum of synthesized silica xerogel.

4.3.2 Hydrocortisone analysis

Hydrocortisone used in this study was also analyzed by FTIR for reference purposes. Figure 4.11 shows the FTIR spectrum result of that analysis. Wave number peak values were noted and their transmission values were compared to literature as shown in Table 4.6.

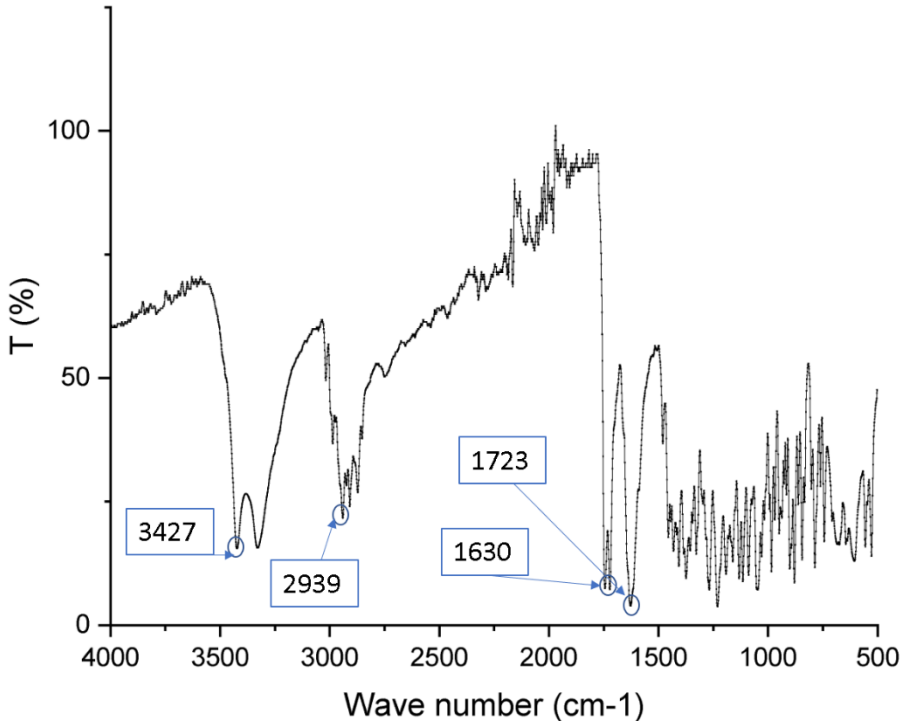

Figure 4. 11: FTIR spectrum of Hydrocortisone.

Table 4. 6: FTIR spectrum report summary.

Wave number (cm^{-1})	T (%)	T (%) in literature
3427	16	17
2939	22	35
1723	8	11
1630	4	4

Wave number 3427 cm^{-1} indicate an O-H Stretching while, 2939 cm^{-1} describes a CH_3 asymmetrical stretching.1723 cm^{-1} describes a C=O stretching and 1630 cm^{-1} is aromatic C=C stretching and lastly an out of plane bending of the ring C-H is described by the low-frequency range between 900 and 600 cm^{-1}(Manivannan et al., 2018).

4.3.3 PVA/Hydrocortisone analysis

PVA/Hydrocortisone electrospun samples were also analyzed with FTIR. The aim of the analysis was to confirm the existence of the hydrocortisone in the samples as the SEM/EDAX analysis was not conclusive enough. Needless to say, the result of the analysis (Figure 4.12) when compared to pure PVA fibers (Figure 4.13) shows the existence of hydrocortisone as the out of plane C-H vibration can be seen in the range of 3400 to 3200 cm^{-1}. Furthermore, ring Carbon vibrations can be seen as well in 1700 to 1600 cm^{-1}.

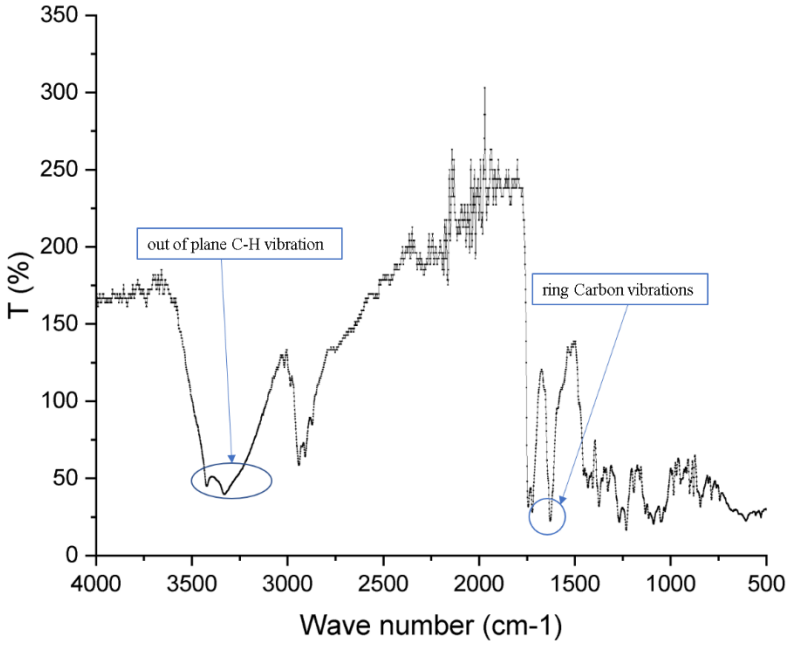

Figure 4.12: FTIR spectrum of PVA/hydrocortisone.

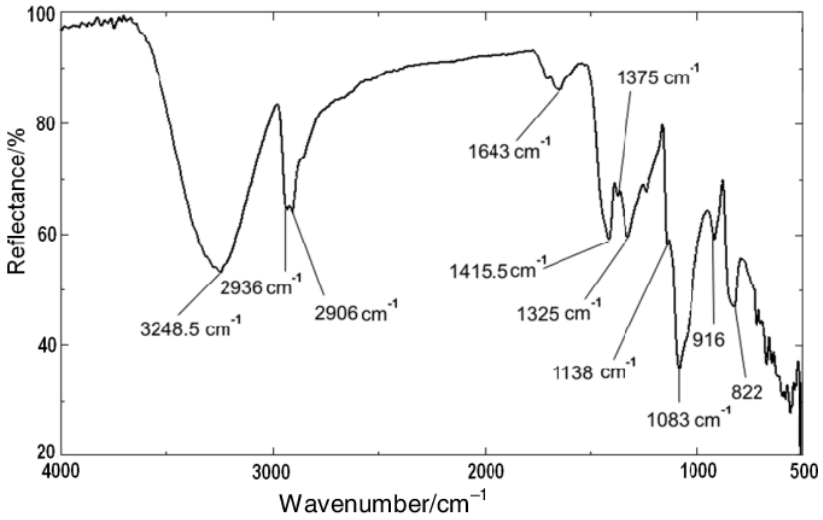

Figure 4.13: FTIR spectrum of pure PVA (Deleanu et al., 2012).

4.3.4 PVA/xerogel/hydrocortisone analysis

Lastly, PVA/xerogel/hydrocortisone electrospun samples were analyzed with FTIR. Figure 4.14 shows the FTIR spectrum of PVA/xerogel/hydrocortisone where Si-O-Si stretching is indicated in the frequency range of 1300 to 800 cm^{-1}. On the other hand, frequency ranging from 3400 to 3200 resemble a C-H vibration. Furthermore, ring Carbon vibrations are indicated in frequency range of 1700 to 1600 cm^{-1}.

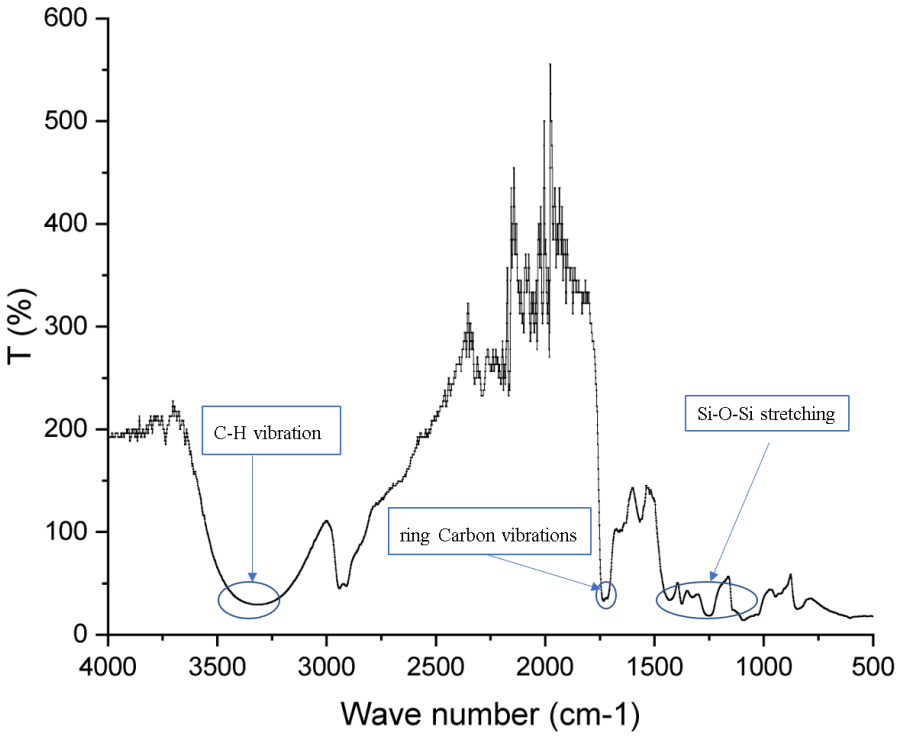

Figure 4.14: FTIR spectrum of PVA/xerogel/hydrocortisone.

4.4 In Vitro Drug Release Analysis

In vitro drug release analysis was performed for hydrocortisone loaded xerogel, PVA/xerogel/hydrocortisone and PVA/hydrocortisone samples. The goal of this analysis was to determine the cumulative hydrocortisone release percentage of each of those samples inside PBS.

4.4.1 Cumulative hydrocortisone release of Xerogel

UV-Vis spectrometry result showed at peak at 280 nm as shown in Figure 4.14. the absorbance value that corresponds with this wave length are summarized in Table 4.7.

Table 4.7: Absorbance values of hydrocortisone loaded xerogel

Time which samples were taken (days)	Absorbance (a.u.)
0	0
1	0.127
2	0.139
4	0.126
8	0.137
16	0.15
25	0.154

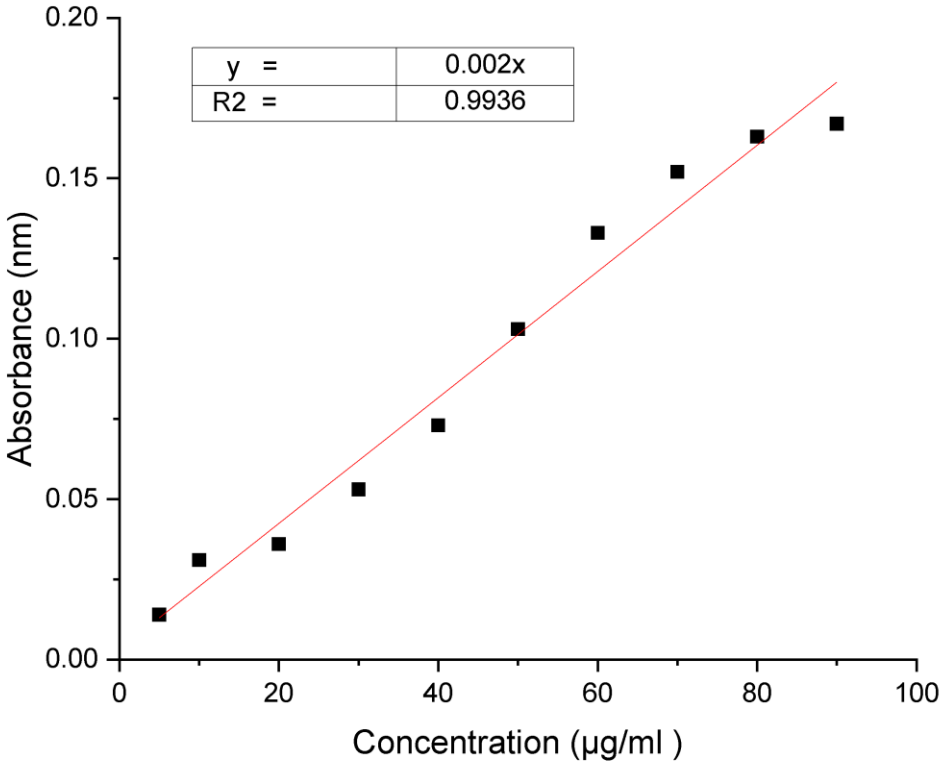

Figure 4.15: Calibration curve of hydrocortisone.

Using the calibration curve shown in Figure 4.15. the concentration of each sample corresponding with recorded absorbance values as well as percentage of the hydrocortisone were calculated. Table 4.8 demonstrates the results. Furthermore, Hydrocortisone **c**umulative release time are demonstrated by the Figure 4.16.

Table 4.8: Hydrocortisone concentration and percentage in hydrocortisone loaded xerogel.

Time which samples were taken (days)	Absorbance (a.u.)	Concentration (μg/mL)	Percentage of drug release (%)
0	0	0	0
1	0.127	5.715	57.15
2	0.139	6.255	62.55
4	0.126	5.67	56.7
8	0.137	6.165	61.65
16	0.15	6.75	67.5
25	0.154	6.93	69.3

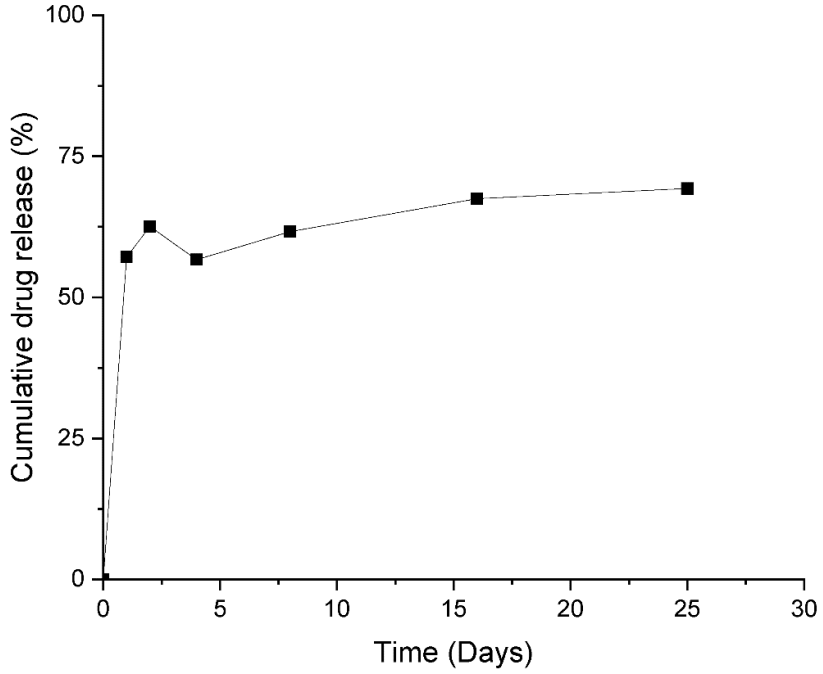

Figure 4. 16: Cumulative drug release time for hydrocortisone loaded xerogel.

Figure 4.16 describes the amount of hydrocortisone released relative to the amount of the hydrocortisone initially loaded into the xerogel. The graph shows that the hydrocortisone was released at a rapid rate from xerogel initially but after that the release got slower and more sustained. After the fourth day the release of hydrocortisone started to increase slowly reaching a peak of 69.3% released by the twenty fifth day. This means that about only 69.3% of the initial amount of hydrocortisone loaded in xerogel was released in around 25 days. The rate of the drug release strongly resembles the sustained/controlled drug release model shown in Figure 2.5.

4.4.2 Cumulative hydrocortisone release of PVA/xerogel/hydrocortisone

UV-Vis spectrometry result showed at peak at 280 nm. The absorbance value that corresponds with this wave length are summarized in Table 4.9.

Table 4.9: Absorbance values of PVA/xerogel/hydrocortisone.

Time which samples were taken (days)	Absorbance (a.u.)
0	0
1	0.127
2	0.12
4	0.127
8	0.165
16	0.17
25	0.176

Similarly, the calibration curve shown in Figure 4.15 was utilized to calculate the concentration of each sample corresponding with its absorbance values as well as percentage of the hydrocortisone. Table 4.10 demonstrates the results. The hydrocortisone cumulative release time were calculated as well and are demonstrated by the Figure 4.17.

Table 4.10: Hydrocortisone concentration and percentage in PVA/xerogel/hydrocortisone.

Time which samples were taken (days)	Absorbance (a.u.)	Concentration (μg/mL)	Percentage of drug release (%)
0	0	0	0
1	0.127	5.715	57.15
2	0.12	5.4	54
4	0.127	5.715	57.15
8	0.165	7.425	74.25
16	0.17	7.65	76.5
25	0.176	7.92	79.2

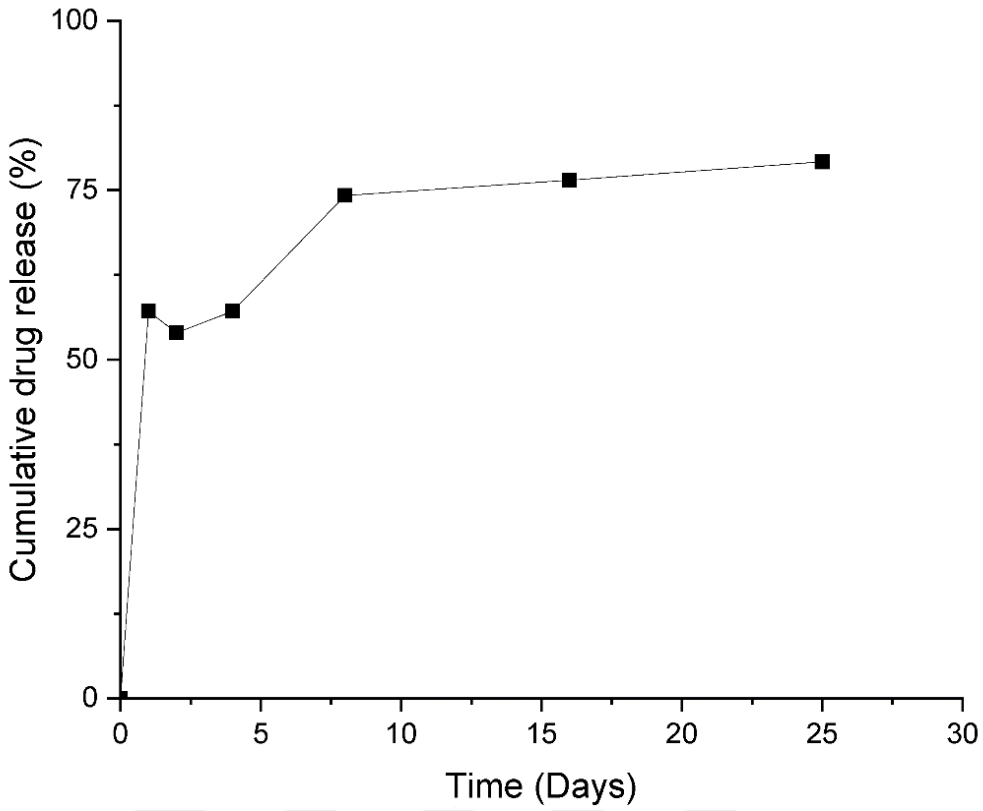

Figure 4.17: Cumulative drug release time for PVA/xerogel/hydrocortisone.

Figure 4.17 describes the amount of hydrocortisone released relative to the amount of the hydrocortisone initially loaded into the PVA/xerogel/hydrocortisone. The graph shows that the hydrocortisone was released at a rapid rate from xerogel initially similar to the xerogel sample. It also follows the same behavior of slowing down release after that to a more sustained release. Similar to the xerogel sample the release of hydrocortisone starts to increase by the fourth day. This time reaching a peak of 79.2% released by the twenty fifth day. This is almost a 10% increase in drug release compared to the xerogel sample.

The graph also indicates that about 79.2% of the initial amount of hydrocortisone loaded in PVA/xerogel/hydrocortisone was released in around 25 days. The rate of the drug release did not deviate much than the xerogel sample which was expected as it is also strongly resembles the sustained/controlled drug release model shown in Figure 2.5.

4.4.3 Cumulative hydrocortisone release of PVA/hydrocortisone

UV-Vis spectrometry result showed at peak at 280 nm. The absorbance value that corresponds with this wave length are summarized in Table 4.11.

Table 4.11: Absorbance values of PVA/hydrocortisone.

Time which samples were taken (minutes)	Absorbance (a.u.)
0	0
15	0.155
30	0.219
60	0.166
120	0.124
240	0.08

The calibration curve shown in Figure 4.15 was used here as well in order to calculate the concentration of each sample corresponding with its absorbancevalues as well as percentage of the hydrocortisone. Table 4.12 demonstrates these results. The hydrocortisone cumulative release time were calculated as well and demonstrated by the Figure 4.18.

Table 4.12: Hydrocortisone concentration and percentage in PVA/xerogel/hydrocortisone.

Time which samples were taken (minutes)	Absorbance (a.u.)	Concentration (μg/mL)	Percentage of drug release (%)
0	0	0	0
15	0.155	6.975	69.75
30	0.219	9.855	98.55
60	0.166	7.47	74.7
120	0.124	5.58	55.8
240	0.08	3.6	36

Figure 4.18 describes the amount of hydrocortisone released relative to the amount of the hydrocortisone initially loaded into the PVA/hydrocortisone. The graph shows that almost all of the hydrocortisone was released from the sample in less than an hour.

This behavior is very different in comparison with the for PVA/xerogel/hydrocortisone and the hydrocortisone loaded xerogel samples. Around 69.75% of the hydrocortisone initially loaded was released in 15 minutes. The release reached a peak of 98.55% released by the 30 minutes mark before the release starts to rapidly slow down.

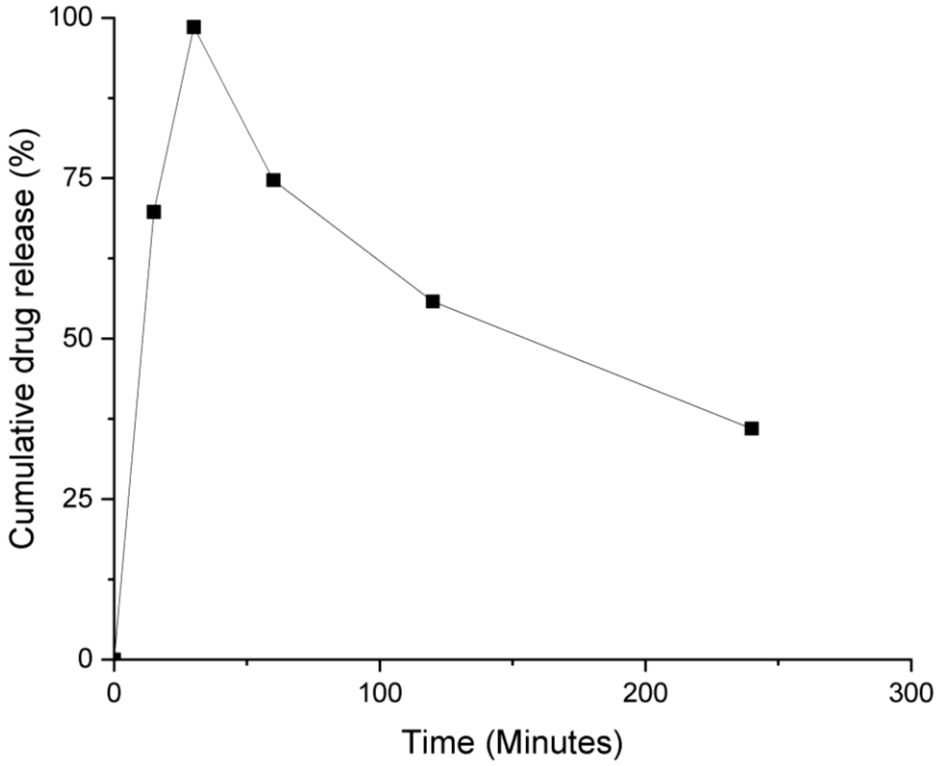

Figure 4.18: Cumulative drug release time for PVA/hydrocortisone.

The graph also indicates that about 98.55% of the initial amount of hydrocortisone loaded in PVA/hydrocortisone was released in the first 30 minutes. The rate of the drug release resembles the conventional/retarded drug release model shown in Figure 2.5.

5. CONCLUSION

This study aimed at the designing and development of hydrocortisone loaded silica xerogel incorporated inside a PVA nanofibrous mat. The drug release behavior of this nanofibrous mat were investigated and compared to the behavior of both silica xerogel alone and PVA loaded with hydrocortisone without silica xerogel. The main outcomes of this study are listed below:

- Silica xerogel was successfully synthesized using TMOS as a silica precursor solution, NH_4OH as a catalyst and Methanol as a co-solvent and it was ball-milled at 30hz for 15-20 minutes in a desk planetary ball miller to reduce its particle size with no negative effects to its properties.
- The synthesized silica xerogel powder had a surface area of 505 m^2/g, pore volume of 0.48 cm^3/g, average pore size of 3.8nm, nanoparticle size of 11.8nm and a median pore width of 0.68nm.
- Two electrospun samples were electrospun; one consisting of PVA loaded with hydrocortisone, the second consisting of PVA and hydrocortisone loaded xerogel and both samples were analyzed using SEM/EDAX , FTIR as well as in vitro dug release.
- SEM results showed the presence of hydrocortisone loaded xerogel in the PVA/xerogel/hydrocortisone while hydrocortisone was hard to detect in the PVA/hydrocortisone sample while, EDAX results indicated the existence of xerogel and hydrocortisone in the PVA/xerogel/hydrocortisone sample as well as the PVA/hydrocortisone sample.
- FTIR analysis showed the presence of an O-H Stretching at wave number 3427 cm^{-1} as well as a CH_3 asymmetrical stretching at 2939 cm^{-1}. in addition to that, C=O stretching and aromatic C=C stretching between 1723 to 1630 cm^1 and lastly an out of plane bending of the ring C-H was found in the range of 900 and 600 cm^{-1}.
- In vitro drug release study for hydrocortisone loaded xerogel showed that that the hydrocortisone was released at a rapid rate from xerogel initially but

after that it the release got slower more sustained with around 60.3% of the initial amount of hydrocortisone loaded in xerogel released in 25 days.

- PVA/xerogel/hydrocortisone showed a similar behavior of that of the hydrocortisone loaded xerogel where the release started at a high pace then slowed to a more sustained release with around 79.2% of the initial amount of hydrocortisone loaded in xerogel released in 25 days.
- On the other hand, PVA loaded with hydrocortisone showed a completely different release behavior. The release stared immediately and around 98.55% of the initial amount of hydrocortisone loaded in PVA released in 30 minutes, resembling a conventional/retarded drug release behavior.
- These results suggest that a PVA/xerogel/hydrocortisone nanofibrous mat are suitable for sustained/controlled topical drug delivery application. It also suggests that the utilization of xerogel inside the nanofibrous mat completely changed the behavior of drug release.

REFERENCES

A.C. Pierre, A. Rigacci. (2011). SiO 2 aerogels, in: N. Leventis, M.M. Koebel (Eds.), Aerogels handbook. Springer Science Business Media LLC. Retrieved July 8 2023, 21–45.

Abdul Khalil HPS, Yahya EB, Tajarudin HA, Balakrishnan V, Nasution H. (2022). Insights into the Role of Biopolymer-Based Xerogels in Biomedical Applications. Gels.; 8(6): 334.Annu. Rev. *Fluid Mech*., 39(1), 217-243.

Arenas, Leliz & Simm, Carolina & Gushikem, Yoshitaka & Dias, Silvio & Moro, Celso & Costa, Tania & Benvenutti, Edilson. (2007). Synthesis of silica xerogels with high surface area using acetic acid as catalyst. *Journal of The Brazilian Chemical Society* - JBCS. 18. 10.1590/S0103-50532007000500003.

Ban, Garram & Song, Sinae & Lee, Hong & Kim, Hee Taik. (2019). Effect of Acidity Levels and Feed Rate on the Porosity of Aerogel Extracted from Rice Husk under Ambient Pressure. *Nanomaterials*. 9. 300. 10.3390/nano9020300.

Beachley V, Wen X. (2010). Polymer nanofibrous structures: fabrication, biofunctionalization and cell interactions. *Prog Polym Sci J 35(7):*868–892.

C. Pereira, A. Matias, M.G. Ventura. (2020). Properties of κ-carrageenan aerogels

C.A. García-Gonz´alez, M. Alnaief, I. Smirnova. (2011). Polysaccharide-based aerogels-Promising biodegradable carriers for drug delivery systems, Carbohydr. *Polym.*86 1425–1438.

C.A. García-Gonz´alez, T. Budtova, L. Dur˜aes, C. Erkey, P. Del Gaudio, P. Gurikov, M. Koebel, F. Liebner, M. Neagu, I. Smirnova. (2019). An opinion paper on aerogels for biomedical and environmental applications. *Molecules*, 24, 1815.

Carlos A. García-González, Alejandro Sosnik, József Kalmár, Iolanda De Marco, Can Erkey, Angel Concheiro, Carmen Alvarez-Lorenzo. (2021). Aerogels in drug delivery: From design to application, *Journal of Controlled Release*. 332, 40-63. Chapter 10 - Pages 337-372.

D.A.S. Agostinho, A.I. Paninho, T. Cordeiro, A.V.M. Nunes, I.M. Fonseca,

David Quintanar-Guerrero, Adriana Ganem-Quintanar, María Guadalupe Nava-Arzaluz & Elizabeth Piñón-Segundo (2009). Silica xerogels as pharmaceutical drug carriers, *Expert Opinion on Drug Delivery*, 6:5, 485-498.

Deleanu, Iuliana & Stoica, Anicuta & M., Stroescu & Dobre, Loredana & Dobre, T. & Jinga, Sorin & Tardei, Christu. (2012). Potassium sorbate

release from poly(vinyl alcohol)–bacterial cellulose films. *Chemical Papers*. 66. 138–143. 10.2478/s11696-011-0068-4.

Dieudonné PH, Hafidi Alaoui A, Delord P, Phalippou J. (2000). Transformation of nanostructure of silica gels during drying. *J Non Cryst Solids*; 262:155-61

Du, A., Zhou, B., Zhang, Z., & Shen, J. (2013). A Special Material or a New State of Matter: A Review and Reconsideration of the Aerogel. *Materials*, 6(3), 941–968.

Ebbell B. (1937). The Papyrus Ebers the greatest Egyptian medical document. Copenhagen: Levin & Munksgaard.

Fernández de la Mora, J. (2007). The fluid dynamics of Taylor cones. *J. Colloid Interface Sci*. 428, 41–48.

Fricke, J. (1988). Aerogels-highly tenuous solids with fascinating properties. *J. Non-Cryst. Solids*, 100, 169–173.

Fricke, J.; Emmerling, A. (1998). Aerogels-recent progress in production techniques and novel applications. *J. Sol-Gel Sci*. Technol, 13, 299–303.

Gersing S, Cagiada M, Gebbia M, et al. (2023) A comprehensive map of human glucokinase variant activity. *Genome Biol*. 24(1):97.

Gesser, H.; Goswami, P. (1989). Aerogels and related porous materials. *Chem*., 89, 765–788.

Guenther U, Smirnova I, Neubert RHH. (2008). Hydrophilic silica aerogels as dermal drug delivery systems – dithranol as a model drug. *Eur J Pharm Biopahrm*; 69:935-42.

Hu X, Liu Sh, Zhou G, Huang Y, Xie Z, Jing X. (2014). Electrospinning of polymeric nanofibers for drug delivery applications. *J Control Release* 185:12–21.

J.C. Wong, H. Kaymak, S. Brunner, M.M. Koebel. (2014). Mechanical properties of monolithic silica aerogels made from polyethoxydisiloxanes, Microporous. *Microporous and Mesoporous Materials*, 183, 23-29.

J.P. Arenas, M.J. Crocker. (2010). Recent trends in porous sound-absorbing materials, *Sound Vib* 44 (7) 12–18.

Janani Balasubramanian, Jack Lemere, S. Sudheer Khan, Nisha Rani Agarwal. (2022). Plasmonic nanosensors and their spectroscopic applications—current trends and future perspectives, Editor(s): V.P. Gupta, *Molecular and Laser Spectroscopy*,

Karout A, Pierre AC. (2007). Silica xerogels and aerogels synthesized with ionic liquids. *J Non Cryst Solids*; 353:2900-9.

Kursawe M, Glaubitt W, Thierauf A. (1998). Biodegradable silica fibers from sols. *J Sol Gel Sci Tech*; 13:267-71.

Lai, C.; Zhong, G.; Yue, Z.; Chen, G.; Zhang, L.; Vakili, A.; Wang, Y.; Zhu, L.; Liu, J.; Fong, H. (2011). Investigation of post-spinning stretching process on morphological, structural, and mechanical properties of

electrospun polyacrylonitrile copolymer nanofibers. *Polymer* 52, 519–528.

M. Salgado, F. Santos, R. Rodriguez-Rojo, R.L. Reis, A.R.C. Duarte, M.J. Cocero. (2017). Development of barley and yeast beta-glucan aerogels for drug delivery by supercritical fluids, *J. CO2 Util*. 22, 262–269.

M. Villegas, A.L. Oliveira, R.C. Bazito, P. Vidinha. (2019). Development of an integrated one-pot process for the production and impregnation of starch aerogels. *Journal of Supercritical Fluids* 154:104592

Manivannan, P., Kumar, R.T., & Periyanayagasamy, V. (2018). SPECTRAL ANALYSIS OF HYDROCORTISONE. *Mesoporous Mater* 183 23–29.

Moghimi H.R., Shafizade A., Kamlinejad M. (2011). Drug delivery systems in Iranian traditional pharmacy (in Persian). Traditional Medicine and Materia Medica Research Center, SBMU, Tehran, Iran.

N. Hüsing, U. Schubert. (1998). Aerogels-airy materials: chemistry, structure, and and Properties. *Angewandte Chemie International Edition*, 37: 22-45

Nautyal, U., ., D., & Gupta, D. (2020). Oral Sustained Release Tablets: An Overview with A Special Emphasis on Matrix Tablet. *International Journal of Health and Biological Sciences*, 3(1), 06–13.

Nayak R, Padhye R, Kyratzis IL, Truong YB, Arnold L. (2011). Recent advances in nanofibre fabrication techniques. *Text Res J 82*(2):129–147.

Nguyen, Hong & T. Hoang, Phuong & Dinh, Ngo. (2018). Synthesis of Modified Silica Aerogel Nanoparticles for Remediation of Vietnamese Crude Oil Spilled on Water. *Journal of the Brazilian Chemical Society*. 29. 10.21577/0103-5053.20180046.

Persano, L., Dagdeviren, C., Su, Y.; Zhang, Y.; Girardo, S.; Pisignano, D.; Huang, Y.; Rogers, J.A. (2013). High performance piezoelectric devices based on aligned arrays of nanofibers of poly(vinylidenefluoride-co-trifluoroethylene). *Nat. Commun*. 4, 1633.

Picollo, M., Aceto, M. & Vitorino, T. (2019). UV-Vis spectroscopy. *Physical Sciences Reviews*, 4(4), 20180008.

Pierre, A.C.; Pajonk, G.M. (2002). Chemistry of aerogels and their applications. *Chem. 102*, 4243–4265.

S. Saeed, R.M. Al-Sobaihi, M.F. Bertino, L.S. White, K.M. Saoud. (2015). Laser induced instantaneous gelation: aerogels for 3D printing, J. Mater. *Chem.* A 3, 17606–17611.

S.S. Kistler. (1931). Coherent expanded aerogels and jellies, *Nature* 127 (3211), 741.

Schaefer, D.W.; Keefer, K.D. (1986). Structure of random porous materials: Silica aerogel. *Phys. Rev. Lett.*, 56, 2199–2202.

Serafin, A.; Murphy, C.; Rubio, M.C.; Collins, M.N. (2021). Printable alginate/gelatin hydrogel reinforced with carbon nanofibers as electrically conductive scaffolds for tissue engineering. *Mater. Sci. Eng.* C, 122, 111927.

Seyedin, Shayan & Mottaghitalab, Vahid & A.K., Haghi. (2008). Evaluation of electrospun nanofiber pore structure parameters. *Korean Journal of Chemical Engineering*. 25. 923-932.

Sharpe, M. (1984). Stray light in UV-VIS spectrophotometers. *Analytical Chemistry*, 56(2), 339A-356A.

Sieminska L, Ferguson M, Zerda TW, Couch E. (1997). Diffusion of steroids in porous sol-gel glass: application in slow drug delivery. *J Sol Gel Sci Tech*; 8:1105-9.

Subramaniam Iswar, Wim J. Malfait, Sandor Balog, Frank Winnefeld, Marco Lattuada, Matthias M. Koebel. (2017). Effect of aging on silica aerogel properties, *Microporous and Mesoporous Materials.* Volume 241, 293-302.

T.A. Esquivel-Castro, M.C. Ibarra-Alonso, J. Oliva, A. Martinez-Luevanos. (2019). Porous aerogel and core/shell nanoparticles for controlled drug delivery: a review, *Mater. Sci. Eng. C Mater. Biol. Appl.* 96, 915–940.

Tamura, T.; Kawakami, H. (2010). Aligned Electrospun Nanofiber Composite Membranes for Fuel Cell Electrolytes. *Nano Lett.*10, 1324–1328.

Vacher, R.; Woignier, T.; Pelous, J.; Courtens, E. (1988). Structure and self-similarity of silica aerogels. *Phys. Rev. B*, 37, 6500–6503.

Verbiˇc, A.; Gorjanc, M.; Simonˇciˇc, B. (2019) Zinc Oxide for Functional Textile Coatings: Recent Advances. *Coatings*, 9, 550.

Wagh, P.; Begag, R.; Pajonk, G.; Rao, A.V.; Haranath, D. (1999). Comparison of some physical properties of silica aerogel monoliths synthesized by different precursors. Mater. *Chem. Phys*., 57, 214–218.

Wang, H.; Niu, H.; Wang, H.; Wang, W.; Jin, X.; Wang, H.; Zhou, H.; Lin, T. (2020). Micro-meso porous structured carbon nanofibers with ultra-high surface area and large supercapacitor electrode capacitance. *J. Power Source*, 482, 228986.

Wang, N.; Zhu, Z.; Sheng, J.; Al-Deyab, S.S.; Yu, J.; Ding, B. (2014). Superamphiphobic nanofibrous membranes for effective filtration of supercritical carbon dioxide, J. *Supercrit. Fluids* 154, 104592. *systems, Mater. Chem. Phys*. 253, 123290.

Yang X, Guo Y, Han Y, Li Y, Ma T, Chen M, Kong J, Zhu J, Gu J. (2019). Significant improvement of thermal conductivities for BNNS/PVA composite films via electrospinning followed by hot-pressing technology. *Compos* B 175:107070

Z. Ulker, C. Erkey. (2017). An advantageous technique to load drugs into aerogels: gas antisolvent crystallization inside the pores, *J. Supercrit. Fluids* 120, 310–319.

Zahra Mazrouei-Sebdani, Hasina Begum, Stefan Schoenwald, Kirill V. Horoshenkov, Wim J. Malfait (2021) A review on silica aerogel-based materials for acoustic applications, *Journal of Non-Crystalline Solids*,562,120770.

Zhang, W.; Zhang, G.; Lu, X.-A.; Wang, J.; Wu, D. (2021). Cellulosic nanofibers filled poly(-hydroxybutyrate): Relations between viscoelasticity of composites and aspect ratios of nanofibers. *Carbohydr. Polym.*, 265, 118093.

CURRICULUM VITAE

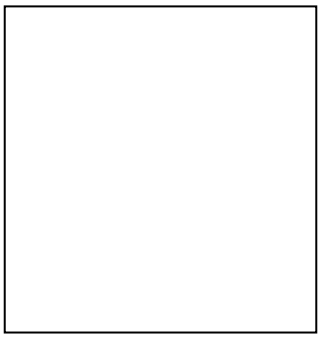

Name Surname **:** Hisham Ali Muhammad Ali MOUSSA

Place and Date of Birth **:**

E-Mail **:**

EDUCATION **:**

- **B.Sc.** **:** 2018, Alexandria University, Engineering Faculty, Textile Department

PUBLICATIONS, PRESENTATIONS AND PATENTS ON THE THESIS:

- **Moussa, H.,** B. Kayaoğlu, Ö. Kalaoğlu "Xerogel Loaded with Hydrocortisone for Drug Delivery," *International Textile & Fashion Congress,* Istanbul, Turkey, March 2023.